



FACULTY OF BIOSCIENCE ENGINEERING

Academic year of 2011-2012

**Structure development in
confectionery products:
importance of triacylglycerol
composition**

Jean Santos

Promotor: Prof. dr. ir. Koen Dewettinck

Tutor: Dr. ir. Nathalie De Clercq

The author and promotor give permission to use this thesis for consultation and to copy parts for personal use. Any other use fall under the copyright laws: the source must be correctly specified when results of this thesis are used.

De auteur en promotor geven toelating om deze thesis te gebruiken voor consultatie voor consultatie en om bepaalde te kopiëren voor persoonlijk gebruik. Elk ander gebruik valt onder het auteursrecht: de bron moet uitdrukkelijk en correct vermeld worden als resultaten uit deze thesis worden gebruikt.

Ghent, August 2012

The promotor,

The author,

Prof. dr. ir. Koen Dewettinck

Jean Santos

Work performed under the tutoring of Nathalie De Clercq at Ghent University, under the Erasmus mobility program, for the degree of Mestrado em Biotecnologia: ramo Alimentar at Universidade Aveiro.

Contents

1.	List of abbreviations.....	1
2.	Abstract	2
3.	Introduction	3
4.	Literature Review	4
4.1.	Overview on fats and oils.....	4
4.1.1.	Definition of fats, oils and lipids	4
4.1.2.	Fatty acids	4
4.1.3.	Triacylglycerols.....	4
4.2.	Fat crystallization	5
4.2.1.	Crystallization	5
4.2.2.	Nucleation	6
4.2.3.	Crystal Growth.....	6
4.2.4.	Crystal size and morphology.....	7
4.2.5.	Polymorphism	7
4.2.6.	Basic polymorphs.....	8
4.2.7.	Polymorphism of triacylglycerols	10
4.2.7.1.	Mixed saturated/unsaturated TAG	10
	– Mono acid TAG SatSatSat	10
	– SatSatO and SatOO	10
	– SatOSat.....	10
	– Compound Crystals	10
4.3.	Microstructural development	10
4.3.1.	Phase Behaviour.....	11
4.3.2.	Phase diagrams.....	11
4.3.2.1.	Examples of phase diagrams	12
	– Phase behaviour of PPP/POP	12
	– Phase diagram of POP/PPO	13
	– Phase behaviour of SOS/SSO.....	14
4.4.	Effect of storage on fats and fat-based products	14
4.5.	Fat Migration on fats and fat-based products.....	15
4.6.	Effect of symmetric/asymmetric triacylglycerols	16
5.	Materials and Methods	18

Contents

5.1.	Raw materials and blends.....	18
5.2.	Fatty acid and triacylglycerol composition	18
5.3.	Preparation of the blends.....	19
5.4.	Differential Scanning Calorimetry (DSC).....	19
5.4.1.	Isothermal DSC	19
5.4.2.	Stop-and-return DSC.....	19
5.5.	Solid Fat Content (SFC).....	20
5.6.	X-ray Diffraction (XRD).....	20
5.7.	Microscopic Analysis.....	21
5.8.	Hardness Measurements.....	22
5.9.	Fat migration	22
5.9.1.	Preparation of Hazelnut Filling	22
5.9.2.	Preparation of samples	22
5.9.3.	Analysis of fat migration.....	23
5.9.4.	Melting Profile	23
6.	Results and Discussion.....	24
6.1.	Composition of the starting oils	24
6.2.	Preparation of the blends.....	25
6.2.1.	Fatty acid composition of the blends.....	25
6.2.2.	Triacylglycerol composition of the blends	26
6.3.	Crystallization behaviour	27
6.3.1.	Solid fat content (SFC) analysis.....	27
6.3.2.	Differential Scanning calorimetry (DSC) analysis.....	28
6.3.2.1.	Isothermal DSC	28
6.3.2.2.	Stop-and-return DSC.....	30
6.3.3.	X-ray diffraction.....	33
6.3.3.1.	Small angle X-ray diffraction.....	35
6.4.	Storage experiments	36
6.4.1.	Hardness measurements	36
6.4.2.	Microscopic analysis	39
6.4.2.1.	Comparison between storage temperatures	39
6.4.2.2.	Crystal Growth with time	42
6.5.	Fat migration	46
6.5.1.	Determination of fat migration.....	46
6.5.2.	Melting Profile	51

Contents

7. Conclusion.....	52
8. Further research.....	54
9. References	55
10. Appendices.....	58

List of figures

Figure 1 - Models of stearic acid (a), elaic acid (b), and oleic acid (c) [2]. 4

Figure 2 - Schematic representation of a triacylglycerol [6]. 5

Figure 3 - Picture showing the different growth faces: Flat (F), Kinked (K) and Stepped (S) [13]. 6

Figure 4 - Packing arrangements of triacylglycerols [6]. 8

Figure 5 – Schematic diagrams representing the polymorphs α , β' and β for tristearin [12]. 9

Figure 6 – Diagram representing the monotropic polymorphs of lipids, α , β' and β and their respective melting temperatures, $Tm\alpha Tm\beta'$ and $Tm\beta$ [8]. 9

Figure 7 – Stages in microstructural development [5]. 11

Figure 8 – Phase diagrams of different binary mixtures, monotectic (a), eutectic (b), montectic (c), molecular compound (d) and peritectic (e) [5]. 11

Figure 9 – Phase diagram of α forms in a POP-PPP mixture (a) and phase diagram of POP-PPP mixture [15]. 13

Figure 10 – Phase behavior of stable forms of PPO-PPP mixtures (a) and metastable forms of PPO-PPP mixtures (b). The subscripted C represents the molecular compounds [16]. 13

Figure 11 - Phase behaviour of SOS-SSO mixture. The subscripted C represents the molecular compounds. 14

Figure 12 - Sample of a stearic-based blend with hazelnut filling in a plastic container. 23

Figure 13 – Fatty acid composition of the raw materials, from left to right, fully hydrogenated shea olein (fhSHo), shea stearin (SHs), interesterified shea (stearin) mid fraction (inSHs), high oleic sunflower oil (HOSF). 24

Figure 14 – Triacylglycerol composition of the raw materials, from left to right, fully hydrogenated shea olein (fhSHo), shea stearin (SHs), interesterified shea (stearin) mid fraction (inSHs), high oleic sunflower oil (HOSF). 25

Figure 15 – Fatty acid composition of the blends. 26

Figure 16 – Triacylglycerol composition of the blends. 27

Figure 17 - SFC curves of all the blends at a) 10°C, b) 15°C, c) 18°C, d) 20°C and e) 23°C. ... 28

Figure 18 – Isothermal DSC curve at a) 18°C and b) 23°C for all blends. 29

Figure 19 - - Stop and return DSC curves at a) 15°C, b) 18°C, c) 20°C and d) 23°C for all blends. 31

Figure 20 - Melting profile at 18°C (left column) and 23°C (right column) for blends 1 (a and b), blend 4 (c and d), blend 6 (e and f) and blend 8 (g and h). 32

List of Figures

Figure 21 – WAXD (d values) at 15°C (left column) and at 20°C (right column) for blend 1 (a and b), blend 4 (c and d), blend 6 (e and f) and blend 8 (g and h).	35
Figure 22 - Evolution of the hardness during storage with a) crystallization at 15°C and storage at 18°C, b) crystallization at 15°C and storage at 23°C, c) crystallization at 20°C and storage at 18°C, d) crystallization at 20°C and storage at 23°C.	37
Figure 23 – Hardness values after 2 hours of crystallization at 15 and 20°C.	38
Figure 24 – Microscopic images of all the blends crystallized at 15°C and stored at 18, 20, 23 and 25°C after a storage period of 4 weeks.	40
Fig. 25 – Microscopic images of all the blends crystallized at 20°C and stored at 18, 20, 23 and 25°C after a storage period of 4 weeks.	41
Figure 26 – Microscopic images of all the blends crystallized at 15 and 20°C and stored at 18 and 23°C after a storage period of 1 week.	42
Figure 27 - Microscopic images of all the blends crystallized at 15°C and stored at 18°C.	44
Figure 28 - Microscopic images of all the blends crystallized at 20°C and stored at 18°C.	45
Figure 29 - Overlay of the TAG profile of the hazelnut filling (red), blend 1 (green) and the tempered sample of blend 1 after being stored for 10 weeks at 20°C (blue).	46
Figure 30 - Comparison of the concentration of various triacylglycerols after 16 weeks of storage for blend 1 (a and b), blend 4 (c and d), blend 6 (e and f) and blend 8 (g and h).	48
Figure 31 – [LOO/SOS], [POO/SOS] and [(LOO+OOO+POO)/SOS] in layer 2 as function of storage time for blends 1, 4, 6 and 8 both tempered (T) and untempered (U) at storage temperature of 20°C (a, c and e) and 23°C (b, d and f).	49
Figure 32 - Melting Profile of the blends 24h after being prepared and stored, a) tempered samples stored at 20°C, b) untempered samples stored at 20°C, c) tempered samples stored at 23°C, d) untempered samples stored at 23°C.	50
Figure 33 - Melting Profile of the blends after 16 weeks of storage, a) tempered samples stored at 20°C, b) untempered samples stored at 20°C, c) tempered samples stored at 23°C, d) untempered samples stored at 23°C.	Error! Bookmark not defined.
Figure 34 - Melting profiles at a) 18°C and at b) 23°C.	58
Figure 35 - Melting enthalpy of the blends stored at 23°C.	58
Figure 36 - Melting enthalpy of the blends stored at 20°C.	58

1. List of abbreviations

C16:0	palmitic acid (P)
C18:0	stearic acid (S)
C18:1	oleic acid (O)
C18:2 ω -6	linoleic acid (L)
C18:3 ω -3	α -Linolenic acid
DSC	Differential Scanning Calorimetry
d_r	distance between the reflecting entities
HOSF	High Oleic Sunflower Oil
SHs	Shea stearin
inSHs	interesterified shea (stearin) mid fraction
fhSHo	fully hydrogenated shea olein
GC	Gas Chromatography
HPLC	High Performance Liquid Chromatography
MUFA	Mono Unsaturated Fatty Acids
OOO	Oleic Oleic Oleic TAG
PLM	Polarized Light Microscopy
pNMR	pulsed Nuclear Magnetic Resonance
PUFA	Poly Unsaturated Fatty Acids
SFA	Saturated Fatty Acids
Sat	Saturated
SAXS	Small-Angle X-ray Diffraction
SFC	Solid Fat Content
SHs	Shea stearin
SLS	Stearic Linoleic Stearic TAG
SOS	Stearic Oleic Stearic TAG
SSO	Stearic Stearic Oleic TAG
SSS	Stearic Stearic Stearic TAG
TAG	triacylglycerols
XRD	X-Ray Diffraction
WAXD	Wide-Angle X-ray Diffraction

2. Abstract

The objective of this thesis was to study the effect of the ratio symmetric/asymmetric TAG on the crystallization properties, storage stability and fat migration of fat blends. In order to do that, eight blends with varying ratios of symmetric/asymmetric TAG, but with an equal amount of saturated fatty acids (40%) were prepared. The preparation of the blends involved the mixing of different fractions of shea butter with high oleic sunflower oil. The ratio of symmetric/asymmetric TAG decreased from blend 1 to 8. These blends were crystallized at 15°C and 20°C and stored at various temperatures according to the experiment. The research was divided in four parts: part one focused on the determination of the composition of the starting materials and blends and their preparation, the investigation of the crystallization behaviour of the blends was done in part two while the storage stability was studied in part three, in part four the fat migration from hazelnut filling to tempered and untempered samples of the blends was studied.

The starting materials and blends were characterized in terms of both fatty acid profile (through the use of GC) and TAG composition (through the use of HPLC). Based on the results of the starting materials the eight blends were prepared with different ratios of symmetric/asymmetric TAG. The crystallization behaviour was investigated using pNMR, DSC (both the isothermal and the stop and return method) and XRD. Regarding the DSC, results showed a two-step crystallization for all blends. The stop and return data gave an indication that polymorphic transitions occurred in most of the blends. This was confirmed by WAXD data that demonstrated a polymorphic transition from α to either β' or β for almost all of the XRD experiments done. The storage stability of the blends was studied with hardness measurements and the analysis of the microstructure was done with polarized light microscopy. The hardness measurements showed that there was no direct pattern regarding the evolution of the hardness with time and/or ratio of symmetric/asymmetric TAG. It was observed that the two blends with the highest amount of SSO had the highest value of hardness directly after the crystallization at 15°C and the value drops substantially during storage whether it was stored at 18 or 23°C. The obtained values suggest that no post-hardening occurred. Through polarized light microscopy it was observed that blends 1, 2 and 3 formed big crystals imbedded in a matrix of small crystals, independently of the crystallization and storage temperature. Regarding to the other blends, they presented numerous crystals of very small size and very small gaps between them. In the study of the fat migration it could be observed that excluding blend 1, the effect of tempering on the prevention of the migration of the TAG seemed to be almost negligible. Between all of the blends, the tempered samples of blend 1 were the most effective in preventing the migration of TAG from the hazelnut filling to the stearic-based blend, while the untempered blend 1 was the less effective of them all.

3. Introduction

Fats consist of a mixture of different triacylglycerols and other minor components. They are the main component of many food products and their composition and characteristics are of fundamental importance in order to obtain end products with the desired properties. Fats are particularly important in the production of confectionary products such as chocolates.

The presence of certain TAG and their respective quantities influences the crystallization behaviour of fats which has important implications in the processing and organoleptic properties of end products and in the processing of raw fats such as palm oil and cocoa butter. The polymorphic forms present, the fat crystal network, solid fat content are all factors that lead to changes in the macroscopic properties. Besides that, it is also important to acknowledge how processing conditions such as the temperature, shear rate and storage time can have an effect on fat-based products.

Regarding to fats, the recent trends in the food industry are mostly related to the reduction of the amount of trans fats and saturated fatty acids on foods. Trans fats and saturated fatty acid are some of the main causes of obesity and cardiovascular diseases, which are among the main causes of death in developed countries [1, 2]. In order to tackle those issues without changing the main sensorial properties of the food products, a deeper understanding of the effect of the composition and processing conditions on the properties of fats is needed.

The main objective of this thesis was to study the effect of the ratio of symmetric/asymmetric TAG on stearic-based blends prepared from various fractions of shea butter and high oleic sunflower oil. In order to do that, eight blends were prepared, the ratio of symmetric/asymmetric TAG decreased from blend 1 to 8.

The research for this thesis can be divided in four parts: the study of the composition of the starting oils and blends, the study of the crystallization behaviour of the blends, the study of the effect upon storage and the study of fat migration from hazelnut filling. The first part was done using HPLC and GC, the second was investigated using pNMR, DSC (both isothermal and stop and return) and XRD. Regarding to the storage experiments, analyses were made through hardness measurements and polarized light microscopy, while the fat migration was studied using HPLC and DSC analysis.

Besides the effect of the ratio of symmetric/asymmetric TAG, the effect of crystallization and storage temperature were also assessed.

4. Literature Review

4.1. Overview on fats and oils

4.1.1. Definition of fats, oils and lipids

Lipids are the name given to a group of compounds found in nature based on fatty acids or molecules that are closely related to fatty acids (e.g. fatty alcohols or sphingosine bases) [3].

The group of lipids is divided between oils and fats. The difference between these two subgroups is that the former is liquid at ambient temperature while the latter is solid [3].

4.1.2. Fatty acids

Fatty acids are aliphatic, monocarboxylic acids and in general, the most common fatty acids contain between 8 and 22 carbon atoms (with even numbers of carbon atoms), have a straight chain and may have one or more unsaturated centres, mostly double bonds of *cis* configuration. Regarding the double bonds, these usually occur at certain positions in the carbon chain. Fatty acids can be classified as unsaturated, monounsaturated or polyunsaturated, if they have no, one or more than one unsaturated centres, respectively [3].

Saturated fatty acids have a straight hydrocarbon chain. A trans-double bond is accommodated with little change in shape, but a *cis*-bond introduces a pronounced bend in the chain (Figure 1) [4]. The position of a double bond influences the melting point [5].

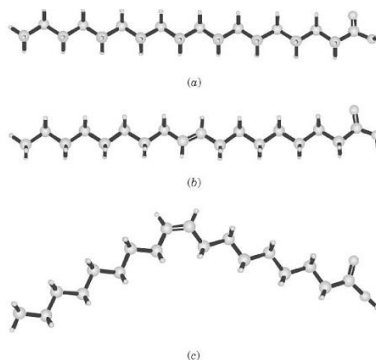


Figure 1 - Models of stearic acid (a), elaic acid (b), and oleic acid (c) [2].

4.1.3. Triacylglycerols

Triacylglycerols are fatty acid tri-esters of glycerol. The fatty acids of the triacylglycerol (TAG) may be all the same, or two may be the same or they can be all different, and the composition of the TAG in terms of its fatty acids will influence its chemical and physical characteristics [5].

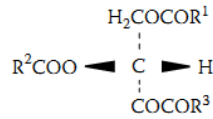


Figure 2 - Schematic representation of a triacylglycerol [6].

In oils of plant origin, unsaturated fatty acids are usually found at the sn-2 position and the more saturated acids are at sn-1 and sn-3 position.

The melting point of a fat or oil increases with the chain length and decreases with number the number of (*cis*) double bonds [3].

Generally the characteristics of a certain fat or oil may be predicted from the composition of the fatty acids present in the triacylglycerols. However, it is important to remember that the properties are dependent of several factors and that oils and fats with similar fatty acid composition can have different melting points, phase behaviours, polymorphic forms, due to the presence of different TAG [5].

4.2. Fat crystallization

The crystallization of fat has a large influence in many properties of a food product like the consistency of high-fat products, the eating properties, the physical stability and also the visual appearance [7].

Fat crystallization must be considered during the processing of lipid products. A proper control of the crystalline microstructure is necessary to obtain products with the appropriate and desired textural and physical characteristics [8].

4.2.1. Crystallization

Crystallization consists in the transition of molecules from a liquid state to a solid state in which the molecules are packed in an orderly and regular manner [9].

The crystallization of a fat is a multi-step process and is a subset of overall solidification, as solids are either crystalline, semicrystalline, or amorphous [10]. In order for crystallization to occur, a sufficiently large thermodynamic driving force should be provided. Thus, supercooling is a prerequisite for crystallizing from a melt.

The thermodynamic driving force is the difference between the chemical potential ($\Delta\mu$) [J/mol] of the liquid phase and the chemical potential of the solid phase. The larger is the difference between the temperature of the crystallizing system and the melting point the larger is the driving force for crystallization [7].

4.2.2. Nucleation

Once a sufficiently large thermodynamic driving force is provided, nucleation occurs and crystals are formed. There are three types of nucleation: primary homogeneous nucleation, primary heterogeneous nucleation and secondary nucleation.

Primary homogeneous nucleation includes the nucleation processes that are not catalysed by fat crystals or foreign solid surfaces. A requirement in order for this kind of nucleation to occur is that the concentration of the solution is higher than the concentration at saturation.

Primary heterogeneous nucleation occurs when foreign surfaces catalyse the nucleation. Comparatively to primary homogeneous nucleation, only a small supercooling is necessary in order for primary heterogeneous nucleation to occur.

Secondary nucleation is due to the existing crystals of the material being crystallised, thus, it can only occur if primary nucleation has already occurred [5]. The existing crystals in suspension lead to the formation of smaller particles and consequently enhance the nucleation rate [11].

4.2.3. Crystal Growth

Crystal growth results from the continuous diffusion of crystallizing molecules to proper places in a growing crystal surface. There are many factors that influence the growth rate. For example the rate of growth is directly proportional to supercooling but is inversely proportional with viscosity. Other factors that influence the growth rate are supersaturation, solvent, temperature and impurities but also the kind of structure, bonds and defects of the crystal [7, 10, 12].

The nature of the interface between the crystal and the liquid determines the mechanism by which the crystal surface grows. The faces may be kinked (K), stepped (S) or flat (F) as illustrated in figure 3 [7].

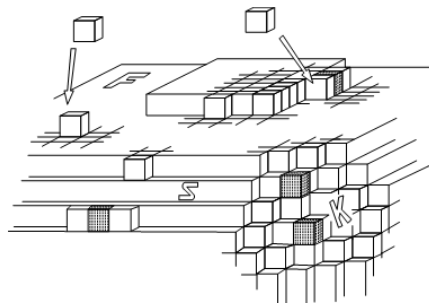


Figure 3 - Picture showing the different growth faces: Flat (F), Kinked (K) and Stepped (S) [13].

4.2.4. Crystal size and morphology

The relative rates of nucleation and crystal growth are responsible for the size of the crystals. Considering that supersaturation has a higher influence on nucleation than crystal growth, the size of the crystals is mainly determined by the rate of nucleation [7].

As the nucleation rate increases with an increasing supersaturation, most of the nuclei are formed when supersaturation is great. In an opposite manner, large crystals are obtained when the supersaturation is low [7].

As nucleation and crystal growth progress, there is a gradual decrease of the supersaturation leading to an increase of the critical size of a stable crystal. This leads to Ostwald ripening, the redissolution of smaller crystals that were stable at higher levels of supersaturation [7].

Regarding the crystal morphology, the relative rates of growth of the different crystal faces may lead to different morphologies.

4.2.5. Polymorphism

Polymorphism is defined as the capacity of a molecule to take more than one crystalline form but yield the same liquid phase when melted [8]. The differences in the hydrocarbon chain packing and variations in the angle of tilt of the hydrocarbon chain packing are what differentiate polymorphic forms in lipids.

Different polymorphic forms have different melting points. Crystalline forms are considered to be enantiotropic when each has a definite range of temperature and pressure in which it is thermodynamically stable. Either of the modifications may be the most stable and transformation can go in both directions, depending on the conditions [7]. To be considered monotropic, one of two crystalline forms must be the most thermodynamically stable form and the other is metastable under all conditions. In this case, transformation can only take place towards the stable form [7].

Polymorphism is influenced by the molecular structure of the triacylglycerol but also by the temperature, pressure, rate of crystallization, impurities and shear rate [8].

Regarding the structure, triacylglycerols can have a double or triple chain-length structure (Figure 4). While the fatty acids of triacylglycerol pairs overlap in the former structure that doesn't happen in the latter.

Generally, double chain-length packing occurs when triacylglycerols with three saturated fatty acids crystallize, while triple chain-length packing is obtained if the triacylglycerol contains fatty acids with different structures, like chain length and unsaturation [8].

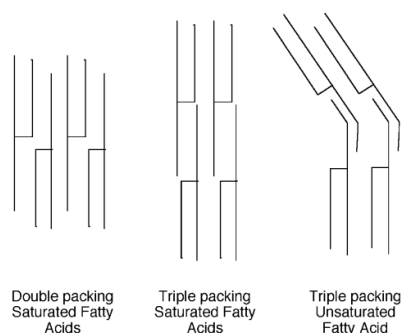


Figure 4 - Packing arrangements of triacylglycerols [6].

4.2.6. Basic polymorphs

To characterize the different polymorphs, the subcell structure is used as the smallest structural unit. The subcell structure refers both to the packing mode of the hydrocarbon chains and the layered structure. The latter results from the repetitive sequence of acyl chains which form a unit lamella [7].

There are three crystallographic types for triacylglycerols: α (alpha), β' (beta prime), and β (beta). These are according to their hydrocarbon subcell packing. The α polymorph is characterized by a hexagonal subcell packing, the chains of the fatty acids are perpendicular to the methyl end group plane. This kind of subcell packing is assumed to have a high degree of molecular freedom. The β' -polymorph has an orthorhombic subcell packing. Here, the fatty acid chains are tilted with respect to the methyl end group plane. Adjacent fatty acid chains are in different planes. The triclinic subcell packing is characteristic of the β -polymorph. In this kind of packing, the fatty acid chains are all in the same plane.

The α form is the least stable polymorph with the lowest melting point and latent heat of fusion, while the β form is the most stable [8]. The hydrocarbon chain packing of the α polymorph is less dense than that of the β polymorph. The denser chain packing of the β polymorph results in an increased stability. The β polymorph has also a higher melting point and higher heat of fusion than α or β' . The order of crystallization of the different polymorphic forms follows the order of their increasing stability, being α the first to crystallize, followed by β' and finally β [8].

Literature Review

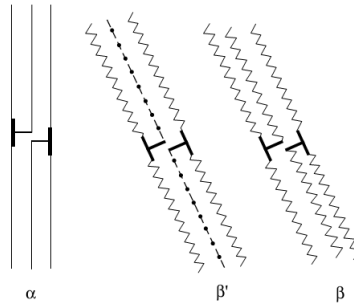


Figure 5 – Schematic diagrams representing the polymorphs α , β' and β for tristearin [12].

Usually the α form is the first to be formed in a rapidly cooled fat, but as it is quite unstable, it quickly transforms to the β' form. As this form is quite stable, it may take a considerable amount of time until it transforms into the most stable β polymorph.

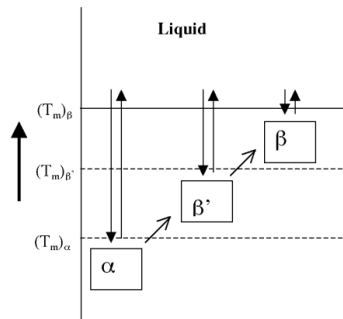


Figure 6 – Diagram representing the monotropic polymorphs of lipids, α , β' and β and their respective melting temperatures, $(T_{m\alpha})$, $(T_{m\beta'})$ and $(T_{m\beta})$ [8].

By using X-ray spectra, the determination of the height of these chair structures and also the distance between the molecules is possible by determining the long and short spacings, respectively [8].

Table 1 - Identification of polymorphic form of fats based on X-ray diffraction analysis [6]

Polymorphic Form	Unit Cell	Lines and Short Spacings (\AA°)
α	Hexagonal	A single strong and very broad @ 4.15
β'	Orthorhombic	Two strong lines @ 4.2 and 3.8
β	Triclinic	A strong line @ 4.6

4.2.7. Polymorphism of triacylglycerols

The main factors influencing which polymorphs exist are the composition and the position of the fatty acids on the glycerol unit.

4.2.7.1. Mixed saturated/unsaturated TAG

- Mono acid TAG SatSatSat

This kind of TAG usually shows three basic polymorphic forms (except when multiple β' -form can occur). The α polymorphic form is detected when cooling the melt. Regarding the β' and β polymorphic, these are obtained via melt-mediated transformation [14].

- SatSatO and SatOO

For this kind of triacylglycerols the β' -polymorph may be the one with the higher stability if the triacylglycerol is asymmetrical. (e.g. SatSatO and SatOO, with S and O standing for saturated and oleic acid, respectively). As the β' -polymorph is less rigorous than the β -polymorphic form, mixed fatty acid TAG tend to be more stable with β' polymorphic form in triple chain length packing [14].

- SatOSat

The SatOSat triacylglycerols have similar polymorphic structures. For example, StOSt has five polymorphs α , γ , β' , β_2 , and β_1 . It is important to mention that the intermediate phase γ can occur. This form has a triple chain-length structure and the saturated and oleic acid chains are disordered [14].

- Compound Crystals

Fats that contain a wider diversity of TAG have the tendency to transform more slowly to stable forms. This is mainly due to the formation of compound crystals. The formation of compound is favoured if the TAG are similar in size, shape and other properties. As compound crystals are not stable, these usually tend to rearrange into purer crystals [14].

4.3. Microstructural development

The microstructural development is divided in three stages: aggregation, network formation, and sintering.

The aggregation of particles occurs randomly, particles encounter each other and then stick together. This last occurrence is responsible for the formation of fractal aggregates [7]. The second stage initiates when the volume fraction of particles in these aggregates is similar to the volume fraction of particles in the system, a continuous network or a gel is beginning to form.

This network is responsible for giving the fat elastic properties [7]. The further crystallisation process leads to sintering. Sintering is the formation of solid bridges between aggregated crystals and aggregates. The formation and properties of a fat crystal network is mainly affected by temperature, concentration and agitation [7].

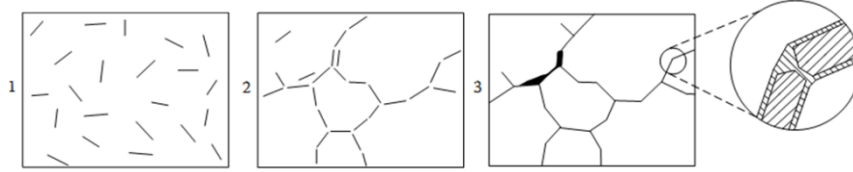


Figure 7 – Stages in microstructural development [5].

4.3.1. Phase Behaviour

A phase is a region of a material throughout which all physical properties of a material are uniform, i.e. there is chemical uniformity and it is physically different from another phase [15].

In the case of natural fats, they contain at least two phases: a liquid and a solid phase. However they usually have more than one solid phase while there is only one existing liquid phase.

4.3.2. Phase diagrams

At constant pressure, a phase is defined by its composition and temperature. Thus, a phase diagram is composed of the temperature on one axis and the composition on the other. Phase diagrams are usually for binary mixtures. For these, five types of diagrams are usually observed.

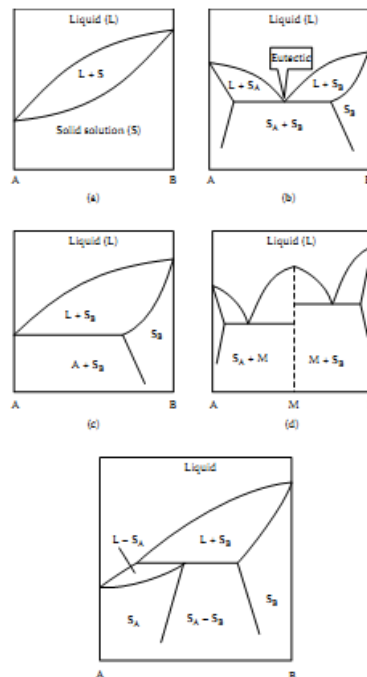


Figure 8 – Phase diagrams of different binary mixtures, monotectic (a), eutectic (b), montectic (c), molecular compound (d) and peritectic (e) [5].

From figure 8a, it can be seen a typical diagram for a monotectic continuous solution, in which triacylglycerols A and B are able to mix and form a continuous solid solution. This usually happens when the two TAG have similar properties (e.g. melting point, polymorphic behaviour, similar fatty acid composition and position) [7].

In figure 8b it is represented a diagram for an eutectic behaviour. Due to the fact that A and B have less similar properties, the solubility of one in the other is limited. This results in a mixture of solid solutions and a sharp decrease and interruption of the liquid line at the eutectic point [7].

In figure 8c there is a shift from the eutectic system to a monotectic. This is triggered as the difference in the melting points of the TAG increases. In this kind of system, the solid high melting TAG dissolves a substantial quantity of the low melting TAG.

In figure 8d A and B may combine to form a molecular compound (represented with M). The molecular compound behaves like a new, pure TAG. Thus, it has unique properties and the diagram resembles two eutectic phase diagrams.

Peritectic systems like the one represented in figure 8b occur usually when saturated and unsaturated systems are mixed, where at least one TAG has two unsaturated acids.

It is important to keep in mind that natural fats have usually more than two TAG, and in order to represent a phase diagram for this kind of fats it should be added one extra axis for each extra TAG. A real fat also doesn't have a unique melting point and there is no precise eutectic point.

4.3.2.1. Examples of phase diagrams

– Phase behaviour of PPP/POP

From figure 9, it can be seen the phase diagrams for PPP/POP mixtures of stable forms (a) and metastable forms (b). According to the graph, it can be observed that for the whole range of POP concentration a monotectic phase was formed for α .

For temperatures below 20 °C, the α forms of both PPP and POP coexist across the whole range of POP concentration. When POP predominates, it can be seen that there is a successive transformation of the POP fraction from α to β' and from β' to β [16].

There are two factors that demonstrate that the PPP-POP mixture is monotectic. The first one is due to the melting point difference between the two components, the difference is about 30 °C. Secondly, the chainlength structure is different, as POP β_2 has a triple structure and PPP β has double structure [16].

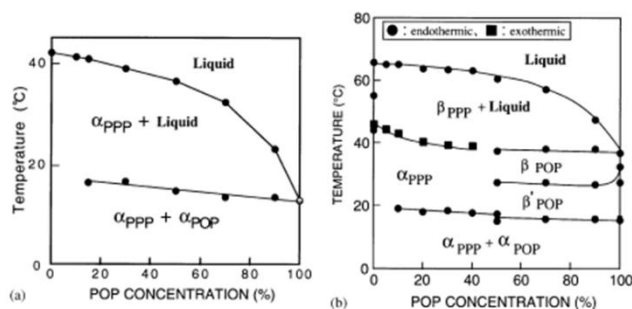


Figure 9 – Phase diagram of α forms in a POP-PPP mixture (a) and phase diagram of POP-PPP mixture [15].

– Phase diagram of POP/PPO

From figure 10, it can be seen the phase diagrams for POP/PPO mixtures of stable phases (a) and metastable phases.

It can be seen from the figure 10 that there is a formation of a molecular compound. According to Himawan et. al [17], this is due to the fact that the two triacylglycerols display a synergistic compatibility and pack more easily together than on their own. This is also observed in other systems in which the two triacylglycerols contain one unsaturated fatty acids like SOS/OSO, SOS/SSO, POP/PPO and POP/OPO. The crystallization rate of compounds is also higher than that of its pure components of the same polymorph [17].

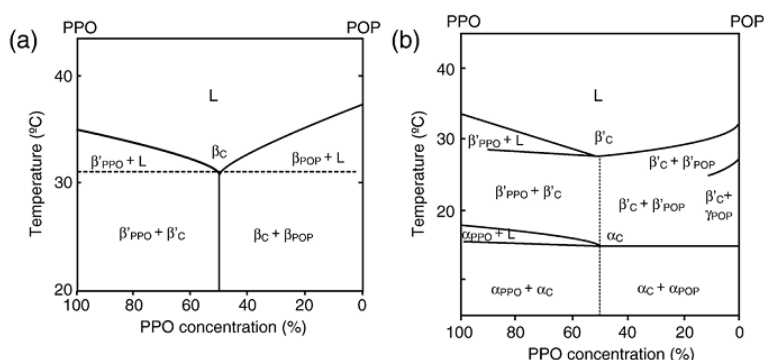


Figure 10 – Phase behavior of stable forms of PPO-PPP mixtures (a) and metastable forms of PPO-PPP mixtures (b). The subscripted C represents the molecular compounds [16].

According to figure 10a, β_C is only formed when the concentration ratio of PPO and POP is 1:1. When the ratio is higher and the temperature is inferior to the melting point of β_C , 31 °C, β'_{PPO} and β_C are present. When the temperature is superior the melting point of β_C , β'_{PPO} and liquid are present.

From figure 10b, it can be observed that the metastable forms of the molecular compound α_C and β'_C are present and are immiscible with the forms of POP and PPO, β'_{PPO} , β'_{POP} , α_{PPO} and α_{POP} [17].

– Phase behaviour of SOS/SSO

As stated on the previous section, the combination of the two triacylglycerols in the two contain one unsaturated fatty acids SOS and SSO display a synergistic compatibility and pack more easily together than individually, leading to the formation of a molecular compound.

Observing the phase diagram below, it can be seen that for concentration of SSO below 35% and temperatures above 39 °C, β_{SOS} is present with liquid. Comparatively, for SSO concentrations above 70% and temperatures above 40 °C, β'_{SSO} is present with liquid. As in the previous situation with POP/PPO, the molecular compound is present when the ratio of SOS and SSO is 1:1 [18].

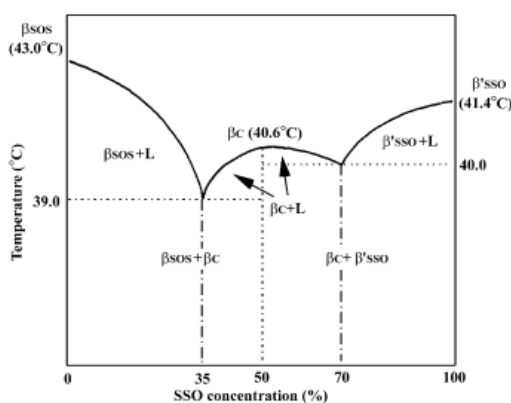


Figure 11 - Phase behaviour of SOS-SSO mixture. The subscripted C represents the molecular compounds.

4.4. Effect of storage on fats and fat-based products

By the moment this thesis was written there were no published studies found about the effect of storage on blends of shea butter. However there are already many published articles focused on the effect of storage on other lipids-based products and blends.

As stated before, many processes can occur after the production of fat blends and fat-based products. Generally those are nucleation, crystal growth, polymorphic transitions, Ostwald ripening, sintering and migration of oil and small crystals.

Regarding to sintering, it is important to keep in mind that in order for the formation of bridges to happen, the polymorphic form of the high melting crystal and the bridge must be the same. The rate of cooling and the temperature gradients also have an important influence on sintering. For example, slow cooling is more favourable than rapid cooling as it prevents the formation of α form which is unable to form bridges with β' or β crystals [19]. The formation of bridges at elevated temperatures is responsible for an increase in the firmness of samples.

As far as the strength of fat crystal networks is concerned, relatively high temperatures during storage can increase the strength as it increases adhesion between partially melted crystals. Also the combined effect of low oil viscosity together with strong adhesion can lead to fat crystal flocculation at elevated temperatures [20].

In the study of Vereecken, et al. [21], it was observed an increase in hardness in some samples during the storage period. Although a higher hardness may be correlated with a crystal network that is more structured and dense, it was seen on the study that samples with similar SFC (solid fat content) values had different hardness values. Consequently, it is important to acknowledge that the strength of a crystal network is due to the solid fat content, but also to the polymorphic behaviour and the size of the crystals. The same study demonstrated that the solid fat content increased during storage, this may result from a rearrangement of the crystals or from a polymorphic transition [21].

In a study with shortenings based with vegetable oil, palm oil and palm kernel oil, there was an increase in the peak melting temperature with storage time and a fractionation was observed in the thermal profiles. This may result from the melting of the low melting TAG when the samples were stored at high temperatures while the high melting TAG crystallized. It was also observed that samples that were stored at higher temperatures had lower SFC values, while samples stored at lower temperatures had higher SFC values [22].

4.5. Fat Migration on fats and fat-based products

Fat migration is a major issue in many food products, mainly in food products in which two components have a different continuous fat phase in contact with each other. Fat migration is the movement of softer fats into harder ones [23, 24].

Although no studies regarding to fat migration on shea butter based blends or products were found by the time this thesis was written, many studies on chocolate or chocolate models can be found.

When chocolate is in contact with some kind of filling (e.g. hazelnut filling), the fat from the filling migrates to the chocolate coating. This leads to an increase in the hardness of the filling and to a decrease in hardness of the chocolate coating as the oil migrates from one phase to the other. Generally, the higher is the quantity of liquid oil in the filling, the greater will be the rate of migration of the oil and the more significant will be the effects on the coating [25].

Although it has been thought for a long time that oil migration happens exclusively due to a diffusion process, some studies questioned if the migration of oil would result from a capillary

flow mechanism instead or even a combination of both. A review article from Aguilera et al. [26] points many evidences favouring the hypothesis that fat might move under capillary forces.

Many factors affect the rate and extension of fat migration. In a study from Ali et al., it was observed that the rate of fat migration in filled dark chocolates that were stored at 30 °C was much faster than the same kind of chocolates stored at 18 °C [27]. A decrease in texture together with a polymorphic transition of the coating from β to β' was also observed in the former samples.

Another study from Depypere et al. found that fat migration in filled chocolates could be delayed when freezed or chilled prior to be stored at 18 °C. It was hypothesized on the same study that the chilling or freezing of the chocolates might have an influence on the diffusion, capillary transport and/or immobilization of the triacylglycerols delaying therefore the fat migration [28].

There are many factors that can influence the rate of fat migration, some of those are: tempering method, cooling rate, content of liquid fat, storage temperature, etc. [29, 30]. It is important however to keep in mind that most of what is known about fat migration is from studies on chocolate models and that the knowledge obtained in this field might or might not be applicable on fat migration on models based on shea butter.

4.6. Effect of symmetric/asymmetric triacylglycerols

The effect of the ratio of symmetric/asymmetric triacylglycerols in blends with the same amount of saturated fatty acids was previously studied by Souleymane and Decock [31, 32]. In both studies, palm-based and stearic-based blends with different ratios of symmetric/asymmetric triacylglycerols were prepared. All blends had the same amount of saturated fatty acids (40%).

Decock found that the SFC curves showed little difference between palmitic and stearic blends, the main differences were found at higher temperatures where solid fat curves of the stearic-based blends had higher values and shifted to higher temperatures. It was found in the same study that at a crystallization temperature of 15°C the blends with higher symmetric/asymmetric TAG ratio crystallized faster for both palmitic and stearic based blends. It was also observed that at a crystallization temperature of 15°C, crystallization during cooling happened for all blends while at 20°C this only happened for the stearic based blends. The DSC data showed a two-step crystallization process for all blends and demonstrated that at lower crystallization temperatures the equilibrium melting enthalpy and melting enthalpy was higher [31, 32].

The data from the XRD showed a polymorphic transition from α to β' for all palmitic based blends while for the stearic based blends a transition from β' to β was observed. This data

Literature Review

corroborates the hypothesis that the crystallization steps observed in the DSC was due to polymorphic transitions [32].

With the hardness measurements, no clear effect of the symmetric/asymmetric TAG ratio was observed. For the stearic based blends, the blend with the intermediate value of ratio of symmetric/asymmetric TAG showed the highest hardness for all storage experiments. Similar observations were made regarding the SFC analysis [32].

Regarding the microstructure, it was observed that the stearic based blend with highest ratio of symmetric/asymmetric TAG had big crystals which were formed within the dense network of small crystals [32]. Souleymane also observed that both the crystallization and storage temperatures could not give a clear and visible effect on the microscopical network, however the storage temperature has a significant effect on the hardness and SFC [31].

It was found that the storage time influenced the hardness and SFC but without any observable trend or evolution, the same regarding the crystal morphology [31].

In general, it can be concluded through those two studies that the higher is the amount of symmetric TAG in a palmitic based blend, the faster will be the crystallization and the earlier will be the induction time. With stearic and mixed blends, because of variable results, there was no clear effect of symmetry. The presence of fatty acids with higher chain lengths have a faster crystallization rate and higher equilibrium melting enthalpy, hardness and SFC [31].

5. Materials and Methods

5.1. Raw materials and blends

All the prepared blends were made by mixing four different raw materials: high oleic sunflower oil (HOSF), interesterified shea (stearin) mid fraction (inSHs), fully hydrogenated shea olein (fhSHo), and shea stearin (SHs), these were main sources of OOO, SSO, SSS and SOS, respectively. The raw materials were provided by Loders Croklaan N.V. (Wormerveer, the Netherlands).

5.2. Fatty acid and triacylglycerol composition

Fatty acid composition was determined by Gas chromatography (GC) producing fatty acid methyl esters (FAME). The procedure involved dissolving one drop (10–20 mg) of sample in 9 mL hexane and reacting with 1 mL 2 N KOH/methanol reagent. After shaking the mixture for approximately 30 seconds it was allowed to settle and 1.5 mL of the hexane layer was then decanted in a GC vial. High-resolution FAME GC was carried out on an Interscience Thermofocus GC with an RTX-2330 column (cyanopropylpolysiloxane, 60 m length, 0.25 mm of internal diameter, 0.2 mm layer thickness) with hydrogen used as a carrier gas. 1 mL of the sample solution was injected via a split/splitless injector (split ratio 20:1) using an autosampler. The oven temperature was programmed starting from 50 °C for 8 min, from 50 to 182 °C at a rate of 5 °C/min, holding then at 182 °C for 20 min, and raising the temperature from 182 to 200 °C at a rate of 5 °C/min and holding again at 200 °C for 5 min. A FID detector was set at 250 °C. Each sample was analysed in triplicate.

The TAG composition of the blends and raw materials was done through High Pressure Liquid Chromatography (HPLC). The analysis were made through two different methods, non-stereospecific and stereospecific analysis. While the former separates the different compounds by their equivalent carbon number (ECN) the former separates by the type and position of the fatty acids in the TAG.

For the preparation of the samples for non-stereospecific analysis, a stock solution of 4 mg/ml was prepared with acetonitrile and dichlorometane in a ratio of 70:30, respectively. Each sample was then prepared from its respective stock solution with a concentration of 0,4 mg/ml.

For the stereospecific analysis, heptane was used as a solvent, which was then diluted to a concentration of 0,5 mg/ml. The procedure was the same as described by De Cock [33]. For both the stereospecific and non-stereospecific analyses, all samples were analysed in duplicate.

5.3. Preparation of the blends

The blends were prepared from the four raw materials previously mentioned. The quantities to add were calculated based on the results from the analysis of the fatty acid and TAG composition of the raw materials.

In order to prepare the blends all the raw materials were melted in the oven at 70°C until they were completely melted. The masses of each raw material were weighed and added to a glass beaker. The mixing was done using a magnetic stirrer equipped with a heating block to prevent crystallization takes place during mixing. The blends were then filled in cups with 15 mL of the blend for the hardness measurement, 3,5 mL of the blends is transferred to NMR tubes for SFC analysis and the rest was stored for other experiments.

5.4. Differential Scanning Calorimetry (DSC)

The study of changes in chemical and physical properties can be done using differential scanning calorimetry (DSC). For this thermo-analytical technique two modes of operation were used: isothermal DSC and Stop-and-return DSC. Both methods were done in a DSC Q1000 (TA Instruments, New Castle, USA) equipped with a refrigerated cooling system (TA Instruments, New Castle, USA) and calibrated with indium (TA Instruments, New Castle, USA), azobenzene (Sigma-Aldrich, Bornem, Belgium) and undecane (Acros Organics, Geel, Belgium). Integrations were done by using the Universal Analysis Software.

5.4.1. Isothermal DSC

Isothermal DSC consists in the isothermal crystallization of fat samples as described by Vereecken et al. [34]. The procedure for the preparation of the samples is the same as described by Foubert et al. [35]. The time-temperature program had the following steps:

1. Holding for 10 minutes at 80°C to ensure that all crystals are melted.
2. Cooling at rate of 25°C/min to the isothermal crystallization temperature either 18°C or 23°C.
3. Holding for 120 min at the isothermal temperature.
4. Heating at 20°C/min to 100°C.

5.4.2. Stop-and-return DSC

Due to the fact that some samples already crystallize during the cooling period of the isothermal DSC, affecting therefore the overall interpretation of the data, the stop-and-return method was used as described by Foubert et al. [36]

Like the isothermal DSC, the sample is first completely melted to remove any fat crystals and is subsequently cooled to the isothermal crystallization temperature. What differentiates the stop-and-return DSC is that the isothermal crystallization is interrupted at different times during the isothermal period and it is melted after repeating another cycle. The melting profiles are integrated and the results are used as a measure of the amount of fat that crystallized at the moment the isothermal crystallization was interrupted. Since different polymorphic forms and fractions have different melting temperatures, the peak temperature gives an idea of the fraction that has crystallized and/or the polymorph in which the fat has crystallized. Measurements were made using crystallization temperatures of 15, 18, 20 and 23°C.

5.5. Solid Fat Content (SFC)

The solid fat content is the mass fraction of solids present at a certain temperature. It was obtained via pulsed Nuclear Magnetic Resonance (pNMR) which measures the solid and liquid signals from the free induction decay (FID) of the samples (as the signals from solids decay faster than signals from liquids it is possible to differentiate them). The SFC is therefore calculated by the ratio between the solid and liquid signals [37].

In order to prepare the samples, the blends were melted at 70°C in the oven (Termaks, Bergen, Germany) to erase all crystal memory, 3,5 mL of sample were then added to each NMR tube (Bruker, Karlsruhe, Germany).

Before each measurement, the pNMR was calibrated with 3 NMR calibration tubes with 0%, 29,8% and 70,8% of solid fat content, respectively. Measurements were made in a Maran Ultra pulsed field gradient NMR (Oxford Instruments, Tubney Woods, Abingdon, UK) and samples were crystallized in a water bath (Julabo F12, Seelbach, Germany).

The isothermal SFC curves were obtained for all the prepared blends during the first 180 minutes. Isothermal curves were measured at 10, 15, 18, 20 and 23°C. All measurements were performed in triplicate.

5.6. X-ray Diffraction (XRD)

The X-ray diffraction is commonly used to identify the polymorphic form of triacylglycerols. In order to convert the unit of the incident angle, θ [°], to the distance between the reflecting entities, d_r [Å], the Bragg's law was used as described below:

$$d_r = \frac{n\lambda}{2 \sin \theta}$$

The order of diffraction, n' [-], is equal to 1. For this work, both wide angle X-ray diffraction (WAXD) and small angle X-Ray diffraction (SAXS) were applied in the analysis of the samples. While the former is used to identify the lateral packing of the fat crystals (α , β' and β), the latter is associated with the long spacings and is used to identify the longitudinal packing of the fat crystals (2L or 3L) [38]

The measurements were performed at the University of Liège, Gembloux Agro Bio Tech, Unité de Valorisation des bioressources, Laboratoire de Science des Aliments et Formulation (Passage des Déportés, 2, B-5030 Gembloux). The measurements were performed with a D8 Advance (Bruker, Germany) with a TTK 450 (Anton Paar), V4 slit, Copper tube and equipped with a Vantec detector (Bruker, Germany). The WAXD analysis was done in the region 15-27° while SAXS measurements were done in the region 1,2-13°.

The temperature program consisted in the following four steps:

1. Heating to 80°C
2. Isotherm for 30 seconds
3. Cooling at 25°C/min to the crystallization temperature (15°C, 20°C)
4. Isothermal period of 120 min.

For the XRD analysis, only blends 1, 4, 6 and 8 were analysed.

5.7. Microscopic Analysis

The microstructure of the fats was analysed via polarized light microscopy (PLM) using a Leitz Diaplan microscope (Leitz Diaplan, Leica, Germany) equipped with a Linkam PE94 temperature control system (Linkam, Surrey, United Kingdom). Pictures of the samples were taken with an Olympus Color View camera (Olympus, Aartselaar, Belgium). The software used was Cell D (Olympus, Aartselaar, Belgium). Images were taken with a magnification of 10x10 (objective and eyepiece).

In order to prepare the samples, the blends were melted in the oven at 70°C, a drop of fat is then transferred to the microscope slide with a pasteur pipette and a cover slip is stacked upon the plate. The samples are then stored in the thermostatic cabinet for crystallization at either 15°C or 20°C during two hours. After the crystallization period is passed the samples are analysed and then stored in the thermostatic cabinet. Samples were stored at 18, 20, 23 and 25°C and pictures were taken at various storage times (day 0, day 1, week 1 and week 4).

5.8. Hardness Measurements

Hardness measurements are quite common in the study of fats and oils as it is useful to assess the macroscopic rheological properties of networks formed by lipids. In this kind of measurement a probe penetrates the samples at a constant speed of 10 mm/min for a distance of 10 mm. the measurement of the maximum load starts as soon as the force of 0,2 N is reached [39].

The samples for the hardness measurement were prepared by filling plastic cups with 15 ml of the samples (five repetitions were made for each sample). Prior to the crystallization, the samples were melted in the oven at 70°C and then put in the water bath at either 15°C or 20°C during two hours. After the crystallization period, the samples were either stored in the thermostatic cabinet at the intended storage temperature (18°C and 23°C) or their hardness was directly determined without storage. Like the microscopic analysis, samples were analysed at various storage times (day 0, day 1, week 1 and week 4).

5.9. Fat migration

The study of fat migration from hazelnut filling to disks of stearic-based blends (tempered and untempered) was assessed during a 16 week period with sampling times after 2, 4, 6, 8, 10 and 16 weeks. The blends 1, 4, 6, and 8 were selected for this experiment and samples were stored in thermostatic cabinets at 20°C and 23°C. All results were compared with the original composition of the respective blend.

5.9.1. Preparation of Hazelnut Filling

The hazelnut filling was prepared using sugar, palm oil and hazelnut mass (45%, 30% and 25% on a weight basis, respectively), the total fat content of the filling was 28%. The filling was prepared by initially mixing all the sugar and hazelnut mass and part of the palm oil (around 12% of the total palm oil used) in a mixer for 20 min at 45 °C. After mixing, the mixture was refined in a three-roll refiner (set at 300-400 rpm) equipped with a water bath at 45°C.

The remaining palm oil was then added to the refined mixture and the final mixture was mixed again.

5.9.2. Preparation of samples

The hazelnut filling was melted at 52°C and 16 g of hazelnut filling was added to each plastic container (cylindrical container with 2,6 cm of diameter and 4 cm of height) by using a dipping bag. The containers with filling were then stored at 10°C in a cooling chamber until the addition of the blends.

For both the untempered and tempered samples 2,5 g of sample were added. For the untempered samples the blends were melted at 70°C in the oven and the fat was directly added to the plastic container with hazelnut filling using a plastic pipette. Regarding the tempered samples, the tempering procedure is similar to the one described by Smith et al. [40], approximately 125 g of melted blend was added to a metal beaker which was cooled and stirred in a water bath at 15°C until it could no longer be stirred effectively. Afterwards, the metal beaker was transferred to another water bath at 36°C and stirred until it was pourable. The tempered blend was then added to the plastic containers with the hazelnut filling using a dipping bag.

For both the tempered and untempered samples the procedure after the addition of the stearic-based blends consisted in placing the samples in a cooling chamber at 10°C for 3 hours and then storing them in the thermostatic cabinet at the storage temperature of either 20°C or 23°C.



Figure 12 - Sample of a stearic-based blend with hazelnut filling in a plastic container.

5.9.3. Analysis of fat migration

At each sampling period five units of each sample were taken and frozen in the freezer for approximately 2 hours. The freezing of the samples was done in order to facilitate the removal of the disk of the blend from the hazelnut filling. These were then cut in the microtome, where the first four layers (counting from the interface with the hazelnut filling) of 750 μm were taken, frozen and stored. Only the second layers were used for the HPLC analysis, the analysis consisted in a non-stereospecific separation of the TAG as described previously. Measurements were done in duplicate.

5.9.4. Melting Profile

After 24h of the preparation of the samples and at each sampling time the melting profile of the samples was obtained through differential scanning calorimetry. The surface of the fat disk was scratched and the fat was sealed hermetically in a DSC pan. The temperature program consisted in setting the initial temperature at 20°C and increasing the temperature at a rate of 5°C/min until 80°C. The software Universal Analysis was used determine the melting enthalpy and peak maxima.

6. Results and Discussion

6.1. Composition of the starting oils

In order to prepare the 8 stearic-based blends with the required 40% of saturated fatty acids and the intended ratio of symmetric/asymmetric triacylglycerols, the fatty acid and triacylglycerol composition of the starting materials had to be determined. fully hydrogenated shea olein (fhSHo), Shea stearin (SHs) and interesterified shea (stearin) mid fraction (inSHs) were mixed with high oleic sunflower oil (HOSF) to prepare those stearic-based blends.

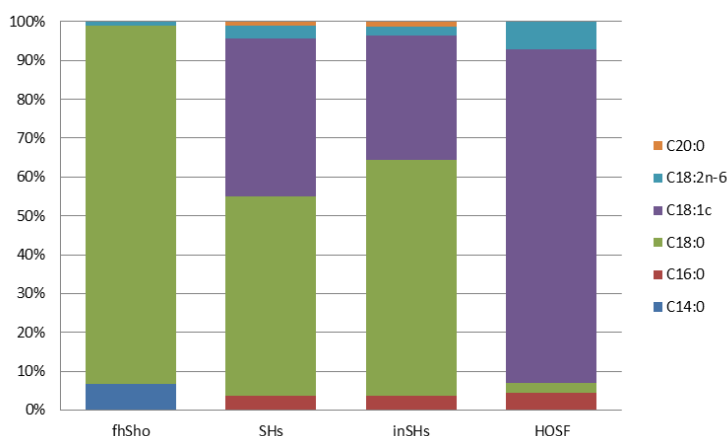


Figure 13 – Fatty acid composition of the raw materials, from left to right, fully hydrogenated shea olein (fhSHo), shea stearin (SHs), interesterified shea (stearin) mid fraction (inSHs), high oleic sunflower oil (HOSF).

The fatty acid composition of the raw materials and blends was determined via GC (see section 5.2). In figure 13, the fatty acid composition of the four starting materials can be analysed. As expected, fully hydrogenated shea olein (fhSHo) has a high content of saturated fatty acids (mostly stearic acid, C18:0, which accounts for 92,2% of all fatty acids) which results from the process of hydrogenation. On the other hand, high oleic sunflower oil (HOSF) has a high amount of unsaturated fatty acids, mainly the monounsaturated oleic acid (C18:1c). Shea stearin (SHs) and interesterified shea (stearin) mid fraction (inSHs) have intermediate concentrations of saturated and unsaturated fatty acids. While SHs has 51,4 and 40,5% of stearic and oleic acid, inSHs has 60,8 and 31,9%, respectively. Except for fhSHo, small amounts of palmitic acid (C16:0) can also be found in SHs, inSHs and HOSF.

Due to the fact that inSHs is a shea stearin mid fraction it has a higher amount of stearic acid than SHs. fully hydrogenated shea olein, interesterified shea (stearin) mid fraction, shea stearin and high oleic sunflower oil had a saturated fatty acid content of 98,9%, 65,8%, 56,2% and 7,0%, respectively.

Results and Discussion

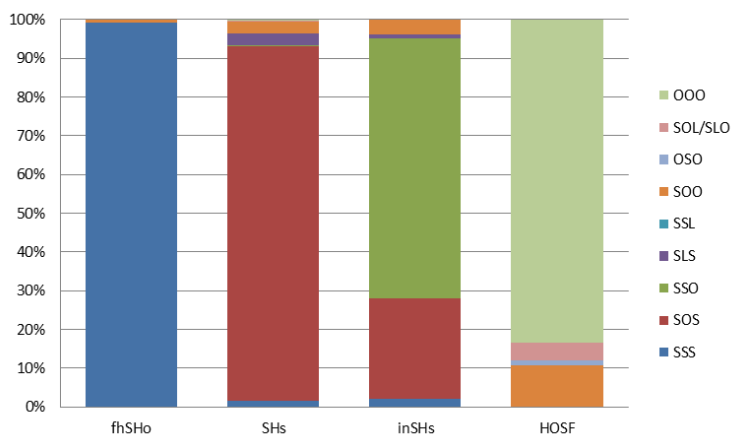


Figure 14 – Triacylglycerol composition of the raw materials, from left to right, fully hydrogenated shea olein (fhSHo), shea stearin (SHs), interesterified shea (stearin) mid fraction (inSHs), high oleic sunflower oil (HOSF).

The triacylglycerol composition of the starting materials was determined via HPLC (see section 5.2) and is presented in figure 14. The high concentration of stearic acid in fhSHo is confirmed by the high content of tristearin (SSS), the presence of other TAG is almost negligible. As expected, inSHs has a high content of SSO compared to SHs which results from the process of interesterification, small amounts of SSS and SOO can also be found in both samples.

The high amount of oleic acid in HOSF is corroborated in the TAG analysis by the high content of triolein (OOO). Also small amounts of SOO and SOL/SLO can be found.

6.2. Preparation of the blends

According to the fatty acid and triacylglycerol composition of the raw materials discussed previously, eight stearic-based blends with 40% of saturated fatty acids were prepared. The blends are numbered from 1 to 8 and have a decreasing ratio of symmetric/asymmetric TAG (i.e. the overall proportion of SSO over SOS increases).

6.2.1. Fatty acid composition of the blends

As it can be seen in figure 15, the fatty acid compositions of the eight blends are quite similar between them. Considering that the main difference between the blends is the ratio of symmetric/asymmetric TAG, no considerable variations should be observed. The saturated fatty acid content ranges from 39,2 to 40,2 %, so there is a very small deviation of the preset 40% SAFA. There are also few variations in the content of MUFAs and PUFAs among the eight

blends.

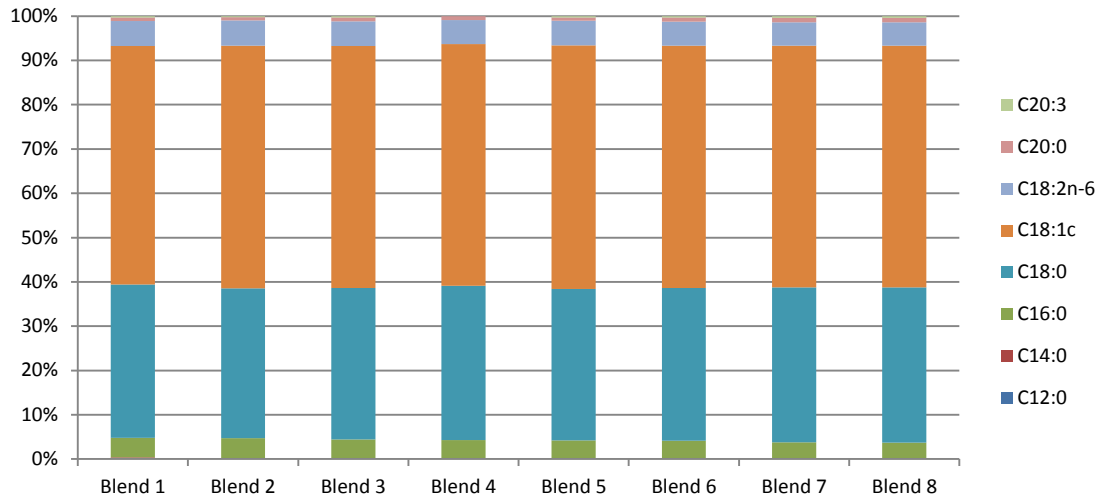


Figure 15 – Fatty acid composition of the blends.

6.2.2. Triacylglycerol composition of the blends

The TAG composition of the blends can be seen in figure 16. All of the blends contain about the same amount of trisaturated TAG (SSS), the same can be observed regarding the triolein content (OOO) and SOO. In general the blends have a similar composition and differ only in the ratio of SOS/SSO. In table 2 the ratios of SOS/SSO are summarized. Due to the fact that no SSO was detected in blend 1, no ratio could be calculated for this sample. As the ratio of blend 6 and 7 is close to one, special attention should be given to those blends as it was reported before that molecular compounds can be formed when similar TAG are present in the same amount [41, 42].

Table 2 - Content of SOS and SSO in all blends and their respective ratio of SOS/SSO.

	Blend 1	Blend 2	Blend 3	Blend 4	Blend 5	Blend 6	Blend 7	Blend 8
SOS	38,1%	36,1%	31,1%	26,6%	22,2%	17,2%	12,8%	8,2%
SSO	0,0%	0,7%	2,4%	4,9%	9,0%	13,1%	18,3%	24,2%
Ratio SOS/SSO	NA	53,3	12,8	5,4	2,5	1,3	0,7	0,3

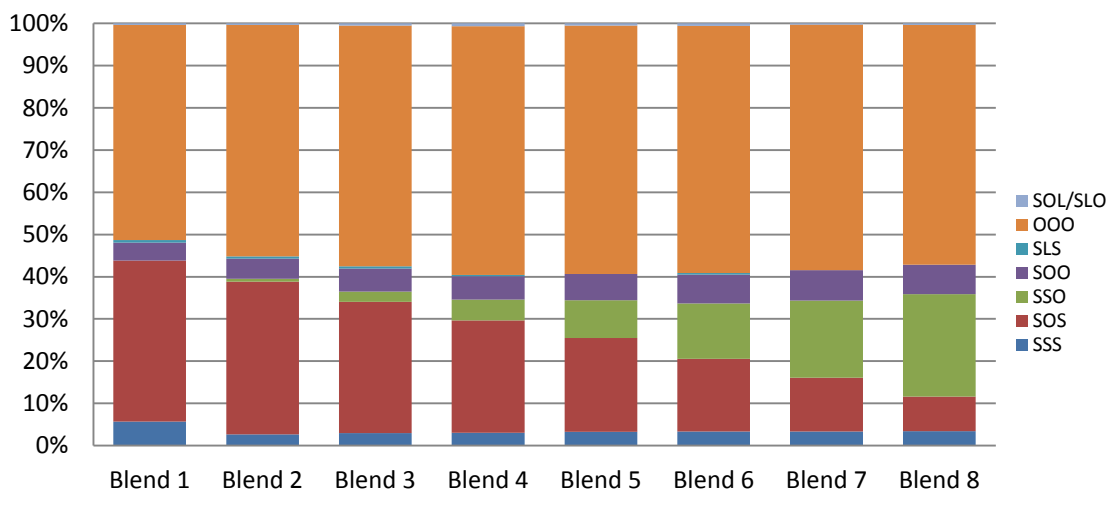


Figure 16 – Triacylglycerol composition of the blends.

6.3. Crystallization behaviour

6.3.1. Solid fat content (SFC) analysis

In figure 17, the evolution of the solid fat content (SFC) with time at various crystallization temperatures can be observed. It is evident the effect of the temperature on the solid fat content, the lower the temperature the higher is the rate of increase of SFC in the first minutes of the experiment, and the higher are the recorded SFC values. While the values of SFC after 180 min for the experiments at 10°C are higher than 50%, no blend presented a SFC higher than 45% at 23°C.

It can be seen in the various figures that there is no clear trend regarding to the rate of increase of SFC and its final value, i.e., there is no observable increase or decrease of the SFC with the increase in the ratio of symmetric/asymmetric TAG. At all temperatures blend 1 presented the highest rate of increase of SFC, followed by blend 2, but no trend is observed after those blends. Similar results were obtained by De Cock [33] for both stearic- and palmitic-based blends.

A two-step crystallization step process can also be observed at the various temperatures. In the first step, the SFC increases almost immediately reaching a first plateau. Afterwards, the SFC increases again in a second step and reaches a plateau again where it stabilizes until the end of the experiment. Factors like polymorphic transformation, fractional crystallization or a combination of both can be responsible for a two-step crystallization process. Data from the X-ray diffraction can give more insights about this process. It is important to notice however, that for blend 1 at 10°C and 15°C and blend 2 at 10°C the process appears to be a one-step crystallization process. This may be due to the fact that the higher amount of SOS may increase the driving force for crystallization. At all temperatures blend 1 and 2 crystallize quicker and reach equilibrium before the other blends.

Results and Discussion

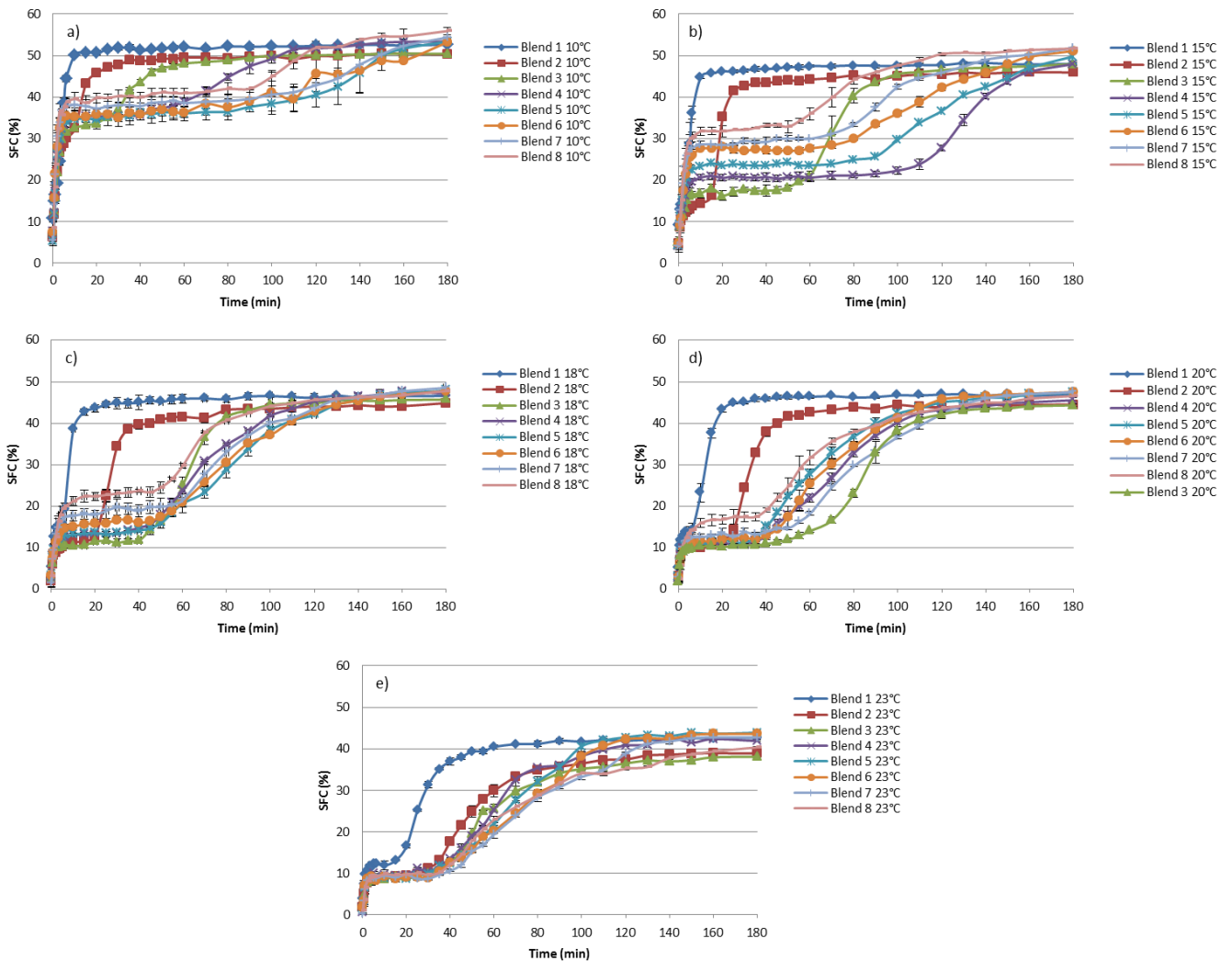


Figure 17 - SFC curves of all the blends at a) 10°C, b) 15°C, c) 18°C, d) 20°C and e) 23°C.

6.3.2. Differential Scanning calorimetry (DSC) analysis

The crystallization behaviour of the blends was studied through the use of differential scanning calorimetry (see section 5.4). Both the isothermal and stop and return methods were used.

6.3.2.1. Isothermal DSC

It can be seen in figure 18 the isothermal DSC of the eight blends at 18°C and 23°C. It appears to happen a shift to higher isothermal times going from blend 1 to 8. However, this shift appears to be much more evident for blends 1, 2 and 3 than for the others. The width of the peaks of blend 1 and 2 is lower than the other blends, this may result from the higher amount of symmetric triacylglycerols which due to their higher melting point results in a higher driving force (the driving force results from the difference between the melting point and crystallization

Results and Discussion

temperature, thus, the higher is the melting point, the higher will be the driving force). The wider composition of the other blends may result in lower melting point and less and less stable crystalline structures leading therefore to the formation of peaks at later times and with increased width in the SFC curve. In the blends that contain SOS and SSO in a ratio close to 1:1 the formation of molecular compounds might be expected, influencing therefore the curves of blend 6 and 7 (which have a ratio of SOS/SSO of 1,3 and 0,7, respectively). In combination with the relatively high amount of the low-melting asymmetric TAG, this could explain the slow crystallization of blend 6, 7 and 8.

Regarding the crystallization at 23°C, a similar trend can be seen but it is evident that the width of the peaks increases. The peak maxima are lower and the time in which the peak maxima occur increases substantially. This could happen because at a higher crystallization temperature the driving force is lower, resulting in the formation of fewer crystals. The increased width of the peaks may result from the longer time the crystallization takes due to the lower driving force.

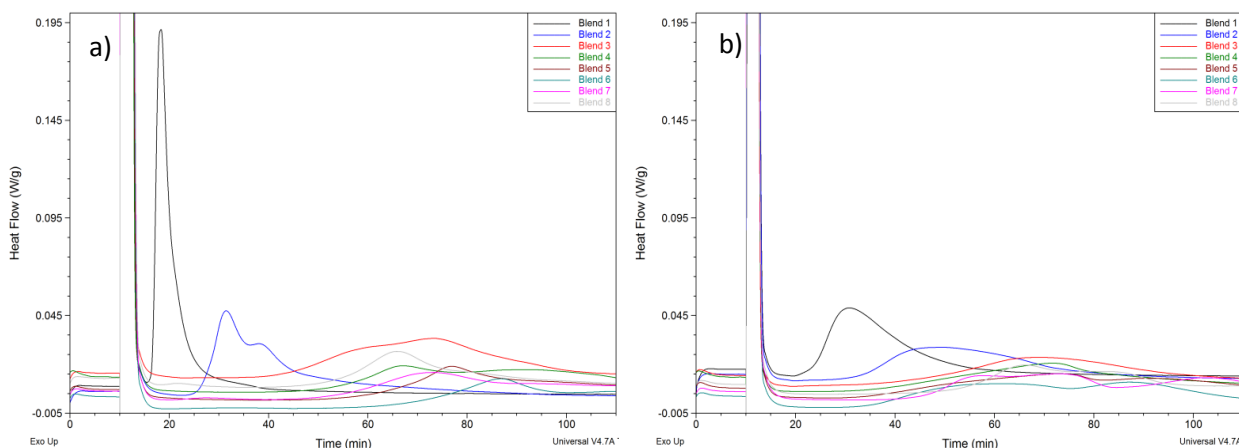


Figure 18 – Isothermal DSC curve at a) 18°C and b) 23°C for all blends.

Both at 18 and at 23°C, only one peak appears for all the blends. Although this may lead to think that a one-step crystallization process occurs in the isothermal period, since the heat flow is no longer zero when the isothermal period begins this suggests that crystallization has already taken place during cooling and the crystallization is therefore a two-step process. This has already occurred before in other studies for both palmitic- and stearic-based blends [34, 43, 44]. A two-step crystallization process can result from either a polymorphic transition to a more stable polymorph or due to fractionated crystallization, where the crystallization of a high melting fraction is followed by the crystallization of the low-melting fraction. The occurrence of the latter is quite common in palm oil [45].

6.3.2.2. Stop-and-return DSC

Because of the crystallization during the cooling period, the analysis of the crystallization of the blends through isothermal DSC is rather limited. In order to obtain more insight over the crystallization process the stop-and-return DSC analysis of the blends 1, 4, 6 and 8 at 15, 18, 20 and 23°C was done. The melting enthalpy at the different periods was determined and is plotted in function of the isothermal time in figure 19.

At any of the temperatures, no blend presented a melting enthalpy of zero at the start of the isothermal period which results from the crystallization of the fat during the cooling. Although, it is evident that the initial value of melting enthalpy is higher at the lower temperatures as also the overall values of melting enthalpy in general.

Independently of the temperature blend 1 crystallizes faster than the other blends, demonstrating that symmetric TAG based blends influence positively the rate of crystallization. Interestingly, blend 1 is followed by blend 8 at the temperatures of 15, 18 and 20°C but not at 23°C. It is difficult to explain these results, considering that blend 8 has a ratio of symmetric/asymmetric TAG relatively close to 1, it may be due to the formation of some molecular compound. According to Engstrom [46], the melting point of the molecular compound of SSO/SOS of the α polymorph is 26°C, which may mean that at 23°C the temperature difference is too close to result in sufficient driving force to form a molecular compound. Another reason may be due to the fact that its composition is not as wide as blend 4 and 6, which avoid the formation of many mixed crystals. The lower melting point of asymmetric TAG compared to symmetric TAG is also an influencing factor, as it affects the driving force. Data from X-ray diffraction may give further insights of these results.

A two-step crystallization process can be observed for all blends which can result from either a polymorphic transition from α to β' or a fractionated crystallization. An exception appears to be blend 1 at 15°C where a single-step process seems to happen. Regarding to the induction times, the induction times of the second crystallization step tend to increase with increasing temperature. This may result from an increase of the rate of polymorphic transition at higher crystallization temperatures

Results and Discussion

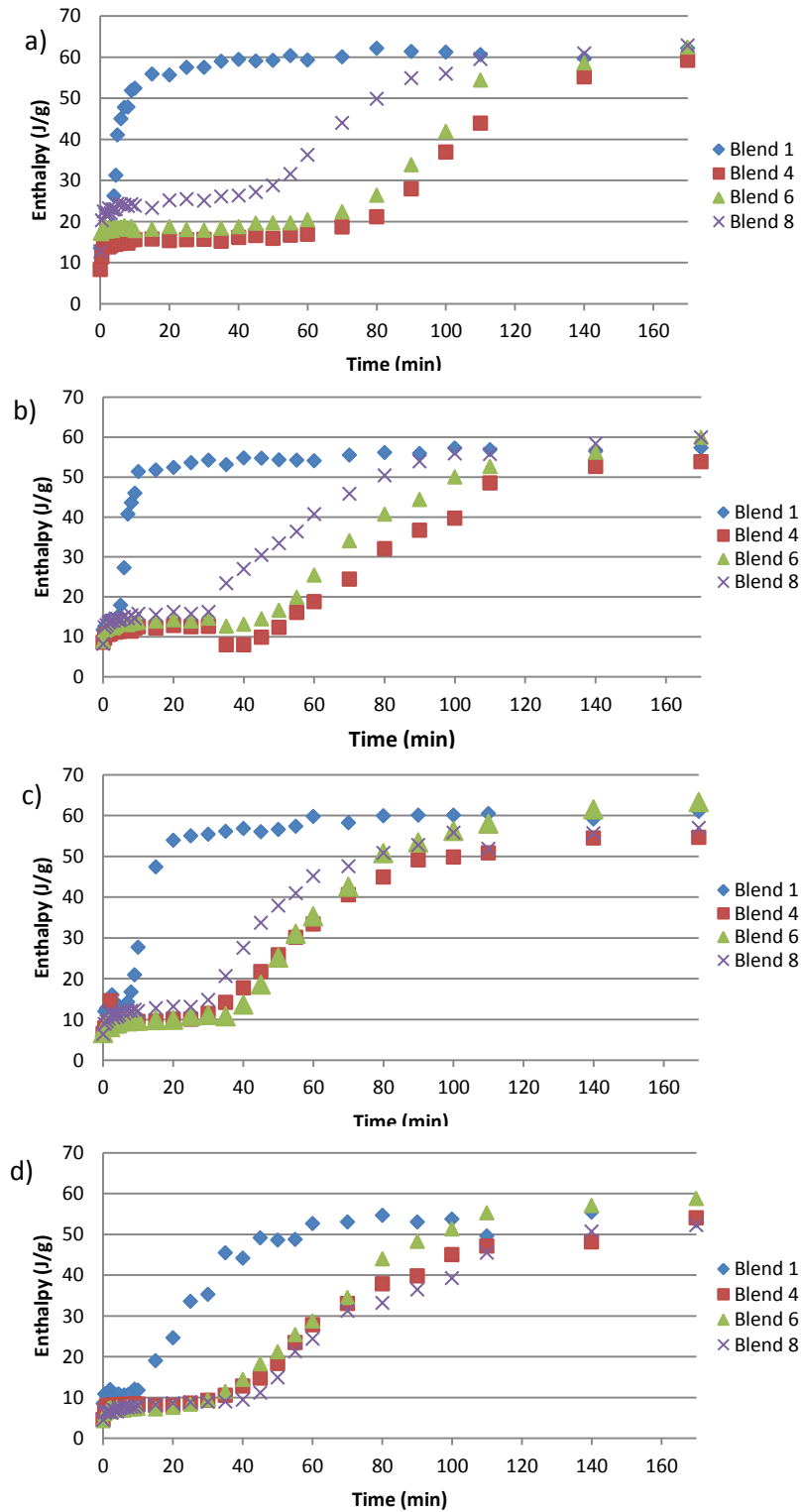


Figure 19 - - Stop and return DSC curves at a) 15°C, b) 18°C, c) 20°C and d) 23°C for all blends.

Results and Discussion

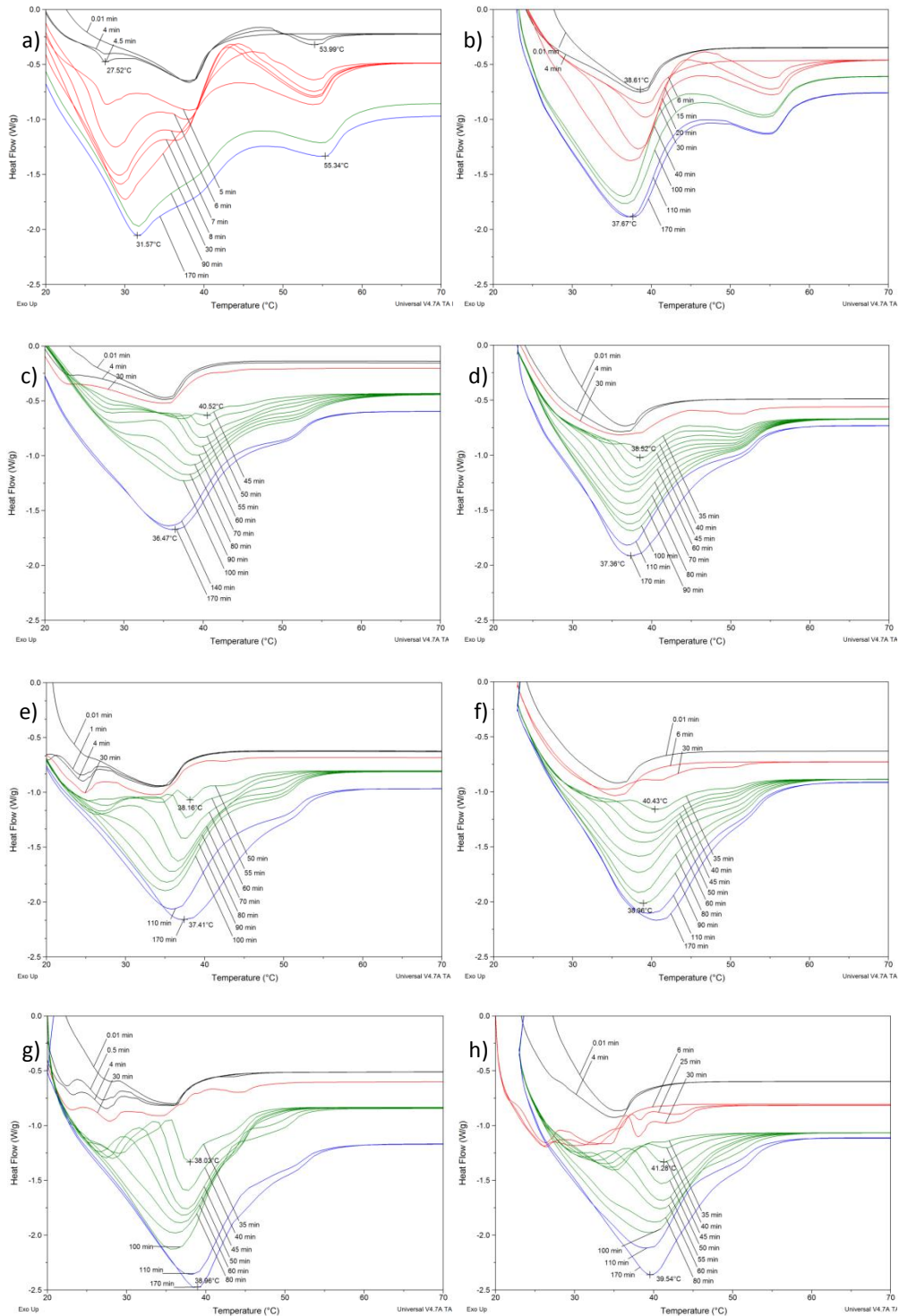


Figure 20 - Melting profile at 18°C (left column) and 23°C (right column) for blends 1 (a and b), blend 4 (c and d), blend 6 (e and f) and blend 8 (g and h).

The analysis of the melting profiles in figure 20 gives more insights about the crystallization behaviour of the blends at 18°C and 23°C. At 18°C only one peak is present at the start for all of the four blends. As the crystallization proceeds a low melting peak at around 25°C appears and increases. While for blend 1 (Figure 20a) this peak continues to increase and the peak maxima shifts from 27,52°C to 31,57°C, for the other blends it gradually disappears. The first peak disappears in the meantime which indicates a fractional crystallization of a high melting (the first peak) and a low melting (the second peak) fraction. The appearance of a recrystallization peak with the consequent formation of a melting peak at 55,34°C may result from a polymorphic transition. The analysis of the data from X-ray diffraction may clarify this observation.

The melting profiles of the blends 4, 6 and 8 at 18°C are quite similar, there is a singular melting peak at the start, which gradually disappears, and the formation of a melting peak at a higher temperature. For the latter peak, there is a shift of the peak maxima as the crystallization proceeds, a shoulder is also observed on the same peak. Blend 6 and 8 also present a small peak at low temperature which gradually disappears this may result from either a polymorphic transition or fractionated crystallization.

The melting profiles of the blends at 23°C look simpler, this already suggests that at higher temperature crystallization is discouraged by the lower driving force. Similarly as at 18°C, all the blends present a first melting peak at the beginning of the process. For blend 1, the first peak grows as the crystallization goes on with a gradual shift on the peak maxima. A recrystallization peak is observed at ca. 45°C which suggests the occurrence of a polymorphic transition. The resulting melting peak occurs at ca. 50°C but not for blends 4, 6 and 8, for these only a slight shoulder appears.

6.3.3. X-ray diffraction

The X-ray diffraction analysis provides unique insights over the crystallization of fats as it can provide unambiguous information about the presence of polymorphs and the occurrence of polymorphic transitions. Blends 1, 4, 6 and 8 were analysed at 15°C and 20°C. The results of WAXD and SAXS are both presented as a three dimensional figure, in which the peak intensity is in the Z-axis, the isothermal time in the Y-axis and the d on the X-axis. As each subcell packing has its unique set of X-ray diffraction line in the wide angle region the identification of the polymorphs is unambiguous.

The results from the WAXD are presented in figure 21. Regarding to blend 1 (figure 21a and b), it can be seen that when at 15°C there is initially a strong peak at 4,15Å that indicates the presence of the α polymorph during the first minutes but it soon disappears and two peaks at 3,9

Results and Discussion

\AA and $4,6 \text{\AA}$ appear, indicating the presence of a β polymorph. At 20°C , there is a peak at $4,15 \text{\AA}$ of the α polymorph during the whole isothermal period and three other small bumps at $3,9$ and around $4,2$ and $4,4 \text{\AA}$ suggesting the formation of a β' polymorph. Considering that at 15°C the driving force is higher it makes sense that a β polymorph forms at such temperature. The lower driving force at 20°C was not enough to occur a transition from the β' to the β polymorph.

At 15°C , only a peak at $4,15 \text{\AA}$ can be observed for blend 4, therefore only the α polymorph occurs during the whole isothermal time. However, when at 20°C , the α polymorph occurs during most of the isothermal time and after some time two diffraction lines appear at $3,8$ and $4,6 \text{\AA}$. There is therefore a polymorphic transition occurring for blend 4 at 20°C to a β polymorph.

Blend 6 shows a similar behaviour at 15°C and 20°C when compared to blend 4 at the same temperature. A peak at $4,15 \text{\AA}$ can be observed, therefore the α polymorph occurs during the whole isothermal time. At later isothermal time a small bump can be observed at $3,8 \text{\AA}$, suggesting the beginning a polymorphic transition to β . Regarding to what happens at 20°C , a diffraction line occurs initially at $4,15 \text{\AA}$, and at later time two diffraction lines appear at $3,8$ and $4,6 \text{\AA}$ and also a small bump at $4,3 \text{\AA}$. The data suggests that a β polymorph is formed after some time at 20°C .

A polymorphic transition from a α polymorph to a β' polymorphic form occurred when blend 8 was crystallized at 15°C . After more than 60 min of isothermal time the peak at $4,15 \text{\AA}$ starts disappearing and two peaks at $3,7$ and $4,2 \text{\AA}$ can be observed. Curiously the crystallization behaviour is unchanged at 20°C occurring also a polymorphic transition from the α to the β' polymorphic form.

When comparing the data for blends 4 and 6 at both 15 and 20°C , it appears that the increase in temperature increases the rate of polymorphic transition from α to β . The same was observed by De Cock [33], with a stearic-based blend with an intermediate ratio of symmetric/asymmetric TAG. The lower temperature of crystallization may lead to a higher degree of crystallization (where both low and high-melting triacylglycerols crystallize) due to the higher driving force in an unstable form and with few or no transition occurring in the period of measurements, while at the higher temperatures less crystallization occurs (only the high melting fraction crystallizes) because of the lower driving force and therefore polymorphic transition can occur faster.

It is evident from these observations that different temperatures and different ratios of symmetric/asymmetric TAG lead to different results as far as the crystallization behaviour is concerned. As expected all blends presented a α polymorph at the beginning of the

Results and Discussion

crystallization and the temperature leads to different rates of polymorphic transitions. This was already suspected from the data obtained through the DSC analysis.

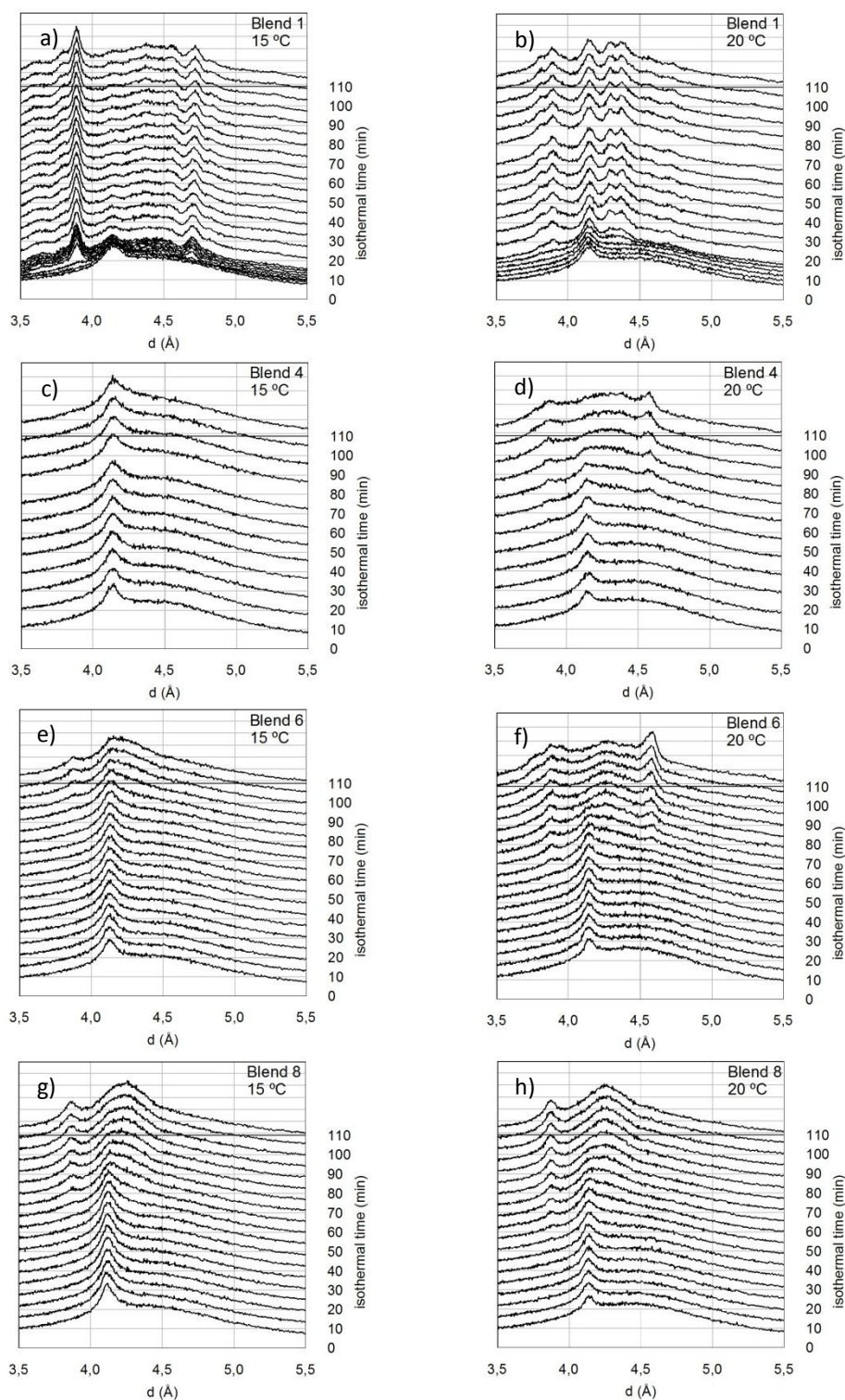


Figure 21 – WAXD (d values) at 15°C (left column) and at 20°C (right column) for blend 1 (a and b), blend 4 (c and d), blend 6 (e and f) and blend 8 (g and h).

6.4. Storage experiments

Factors like the storage time, the storage temperature and the crystallization temperature have generally fundamental factors on the properties of fats and fat products. Through the storage experiments the influence of the previously mentioned parameters on the hardness and microstructure of the fats will be assessed. In order to do so the prepared blends were crystallized at 15 and 20°C and then stored at various temperatures for periods of time ranging from 2 hours to 1 month. The microstructure was analysed via polarized light microscopy while the hardness analysed through the use of a texture analyser. Through all these procedures, the effect of the storage temperature, storage time and ratio of symmetric/asymmetric TAG was assessed.

6.4.1. Hardness measurements

The results of the hardness measurements are presented in figure 22. By observing figure 22a it is clear that there is no direct pattern regarding the evolution of the hardness with time and/or ratio of symmetric/asymmetric TAG. It can however, be observed that the two blends with the highest amount of SSO have the highest value of hardness directly after the crystallization at 15°C and the value drops substantially during storage whether it was stored at 18 or 23°C. Such values suggest that no post-hardening occurs for these blends and the same results are obtained when the blends are crystallized at 20°C. This decrease of hardness with storage time may result from the loss of crystal mass due to dissolving crystals or the loss of strength of the network from Ostwald ripening.

Blends from 1 to 6 show a gradual increase in hardness during the first week when crystallized at 15°C and stored at 18°C, but after such period the hardness drops to values close to the initial ones. When crystallized at the same temperature and stored at 23°C, there is a slight increase in hardness or a decrease in the first day and a gradual decrease in hardness till the end of the experiment. Similarly as for blend 7 and 8 no post hardening occurs for these blends independently of the storage temperature.

The overall effect of the storage temperature on the blends is that there is a decrease in hardness when storing at 23°C when compared to storing at 18°C. This is easily understandable, as the higher is the storage temperature the higher will be the tendency of the fat crystals to melt and higher will be the tendency of the fat crystal network to loosen and decrease its strength. Another observation is that most of the blends were unable to increase their initial hardness value after one month of storage independently of the crystallization or storage conditions. Exceptions include blend 3 and 4 when crystallized at 20°C and stored at 18°C and 23°C.

Results and Discussion

In general, it appears that the blends with the highest amount of SOS (blend 1 and 2) present the lowest values of hardness independently of the chosen crystallization and storage temperatures. Considering that SOS has a lower melting point than SSO [47], it is understandable that hardness values are higher for blends with high content of SOS, as the temperature increases the blends with high SOS content will have a higher tendency to melt leading to the loss of crystal mass due to the dissolution of crystals. Another reason may result from the decrease of the strength of the crystal network due to Ostwald ripening.

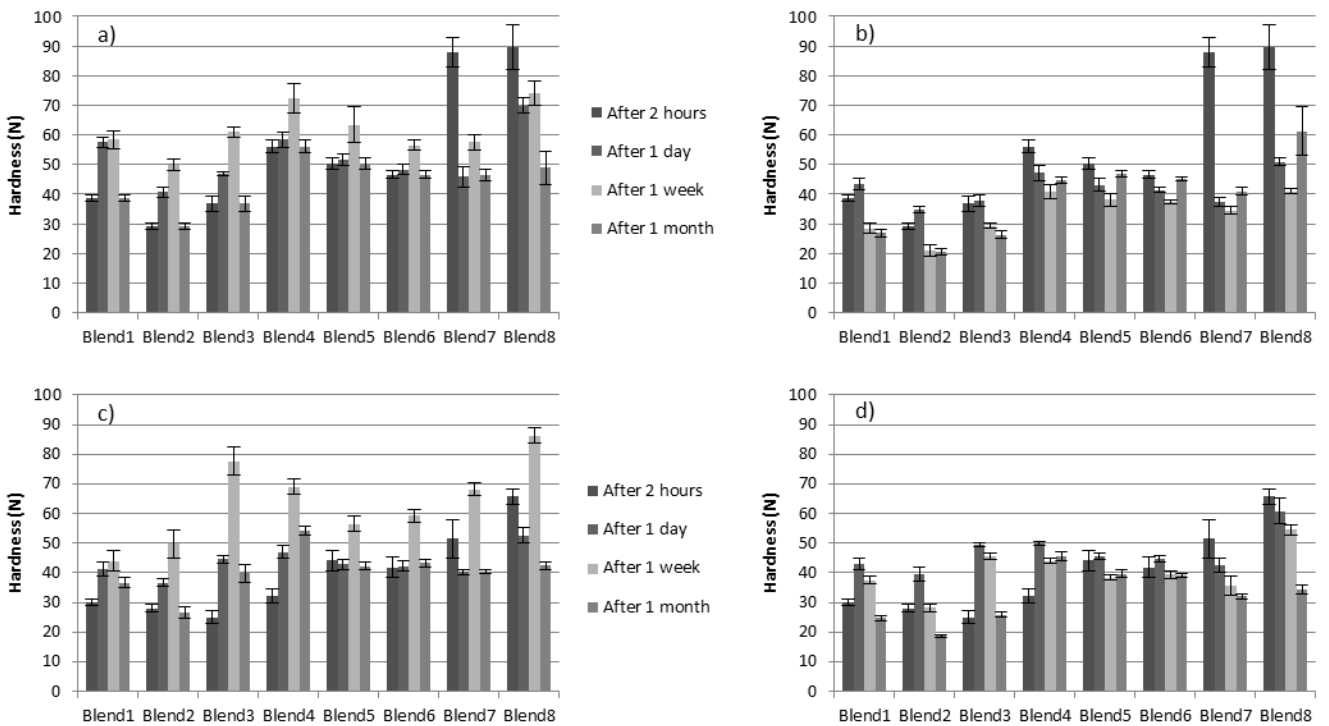


Figure 22 - Evolution of the hardness during storage with a) crystallization at 15°C and storage at 18°C, b) crystallization at 15°C and storage at 23°C, c) crystallization at 20°C and storage at 18°C, d) crystallization at 20°C and storage at 23°C.

6.4.1.1. Comparison between crystallization temperatures

Figure 23 summarizes the hardness values for all the blends directly after crystallization at either 15°C or 23°C.

As stated before, it can be seen that the blends with the highest content of SOS present the lowest values of hardness whether they are crystallized at 15°C or 23°C. On the other hand, blend 7 and 8 which have the highest content of SSO present the highest values of hardness. Therefore, it appears that there is a positive correlation between the content of SSO of a blend and the hardness measured directly after crystallization.

As far as the temperature of crystallization is concerned, hardness values are higher when the crystallization is performed at 15°C. The difference between the hardness values is most evident for blends 7 and 8. A lower crystallization temperature results in a higher temperature drop during the crystallization this favours the occurrence of nucleation over crystal growth, leading therefore to a more dense crystal network which has a big effect on the characteristic of the fat. As it will be observed in the images obtained by polarized light microscopy, blends 1, 2 and 3 (which present some of the lowest hardness values) present a crystal network with large crystal with some gaps between them, while the other blends have a dense crystal network composed of small crystal with no or very small gaps between them.

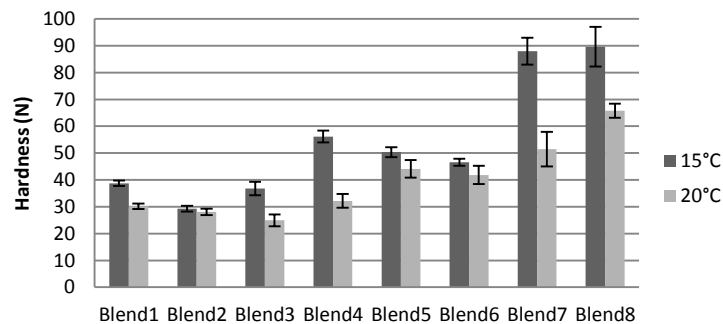


Figure 23 – Hardness values after 2 hours of crystallization at 15 and 20°C.

6.4.2. Microscopic analysis

Through polarized light microscopy (PLM) the effect of storage time and storage temperature was on the fat crystal network was studied. All blends were crystallized at 15 and 20°C and stored at various temperatures.

6.4.2.1. Comparison between storage temperatures

By observing picture 23 and 24 it can be seen that there is some influence of the crystallization and storage temperature on the fat crystal network after 4 weeks of storage. Blends 1, 2 and 3 form big crystals imbedded in a matrix of small crystals, independently of the crystallization and storage temperature. With time, more of the big crystals are formed. However, when these blends are stored at 25°C, they seem to form smaller crystals than when stored at other temperatures.

Regarding to the other blends, their fat crystal network is diametrically different. Instead of being composed of few big fat crystals with wide gaps between them, blend 4, 5, 6, 7 and 8 present numerous crystals of very small size and very small gaps between them. There is therefore a big effect of the amount of the ratio of symmetric/asymmetric TAG on the size and number of the crystals and the density of the fat crystal network. These differences can be observed with any combination of crystallization and storage temperature. It seems therefore that there is a shift on the type of crystal network for blends that had a ratio of SOS/SSO equal and smaller than 6.

As far as the form of the crystals is concerned, it can be seen that blend 1, 2 and 3 form crystals with a spherulitic morphology, which is characteristic of the β' polymorphic form. The spherulitic morphology results from a slow secondary crystallization. The morphology observed for the other blends consists in an amorphous mass of small crystals, that leads to the dense crystal network observed in the images. The β is characterized by the formation of needle-shaped fat crystals [42].

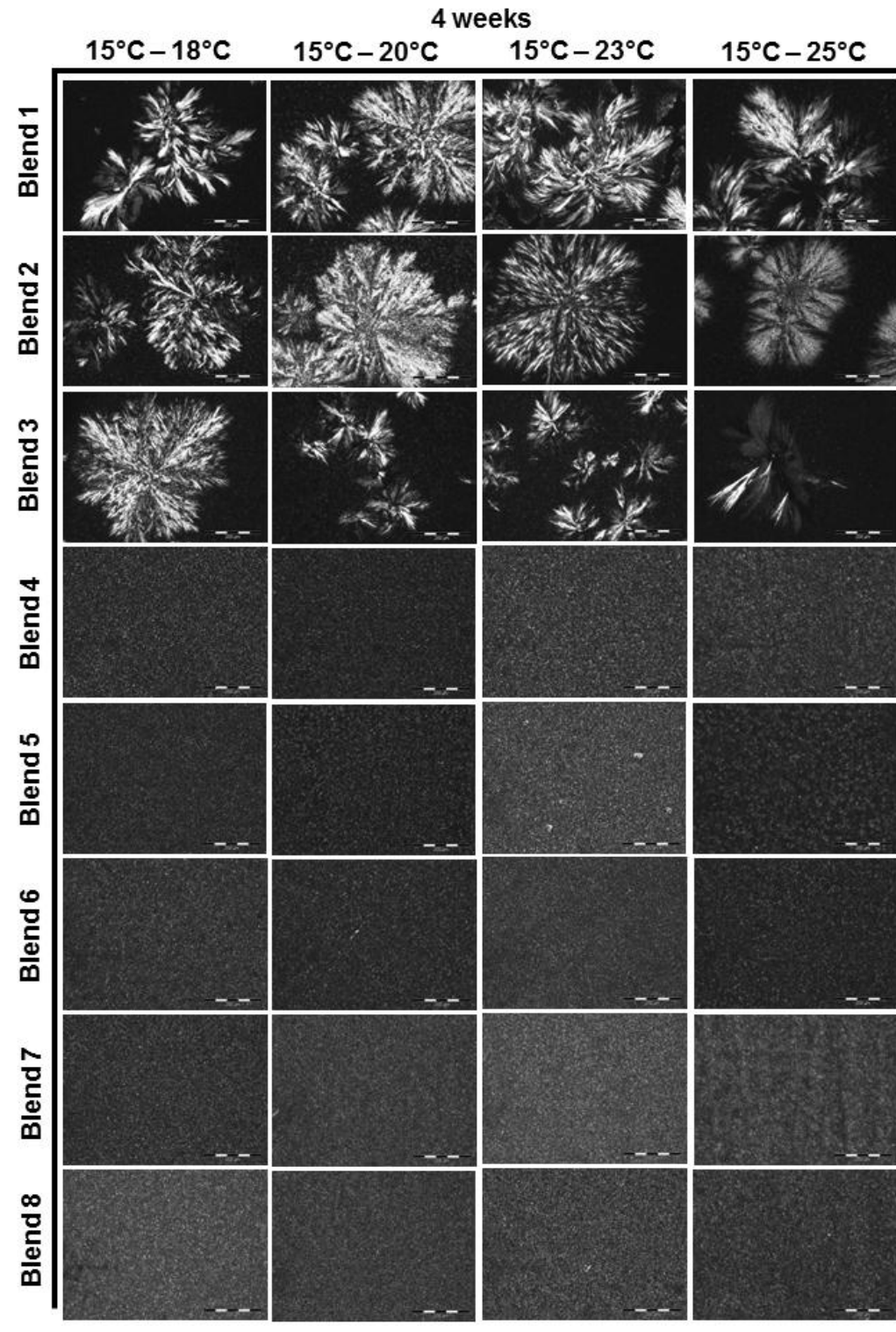


Figure 24 – Microscopic images of all the blends crystallized at 15°C and stored at 18, 20, 23 and 25°C after a storage period of 4 weeks.

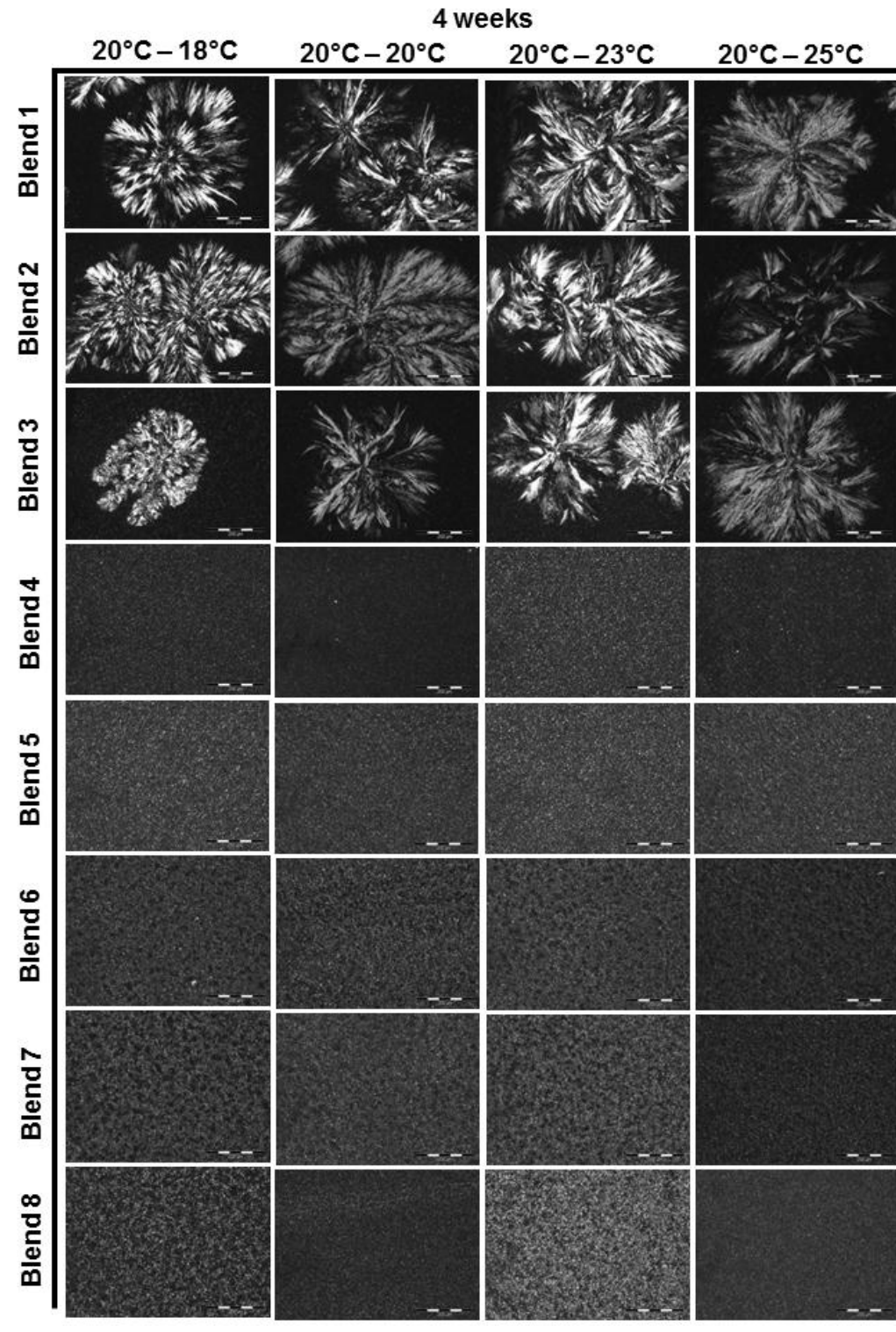


Fig. 25 – Microscopic images of all the blends crystallized at 20°C and stored at 18, 20, 23 and 25°C after a storage period of 4 weeks.

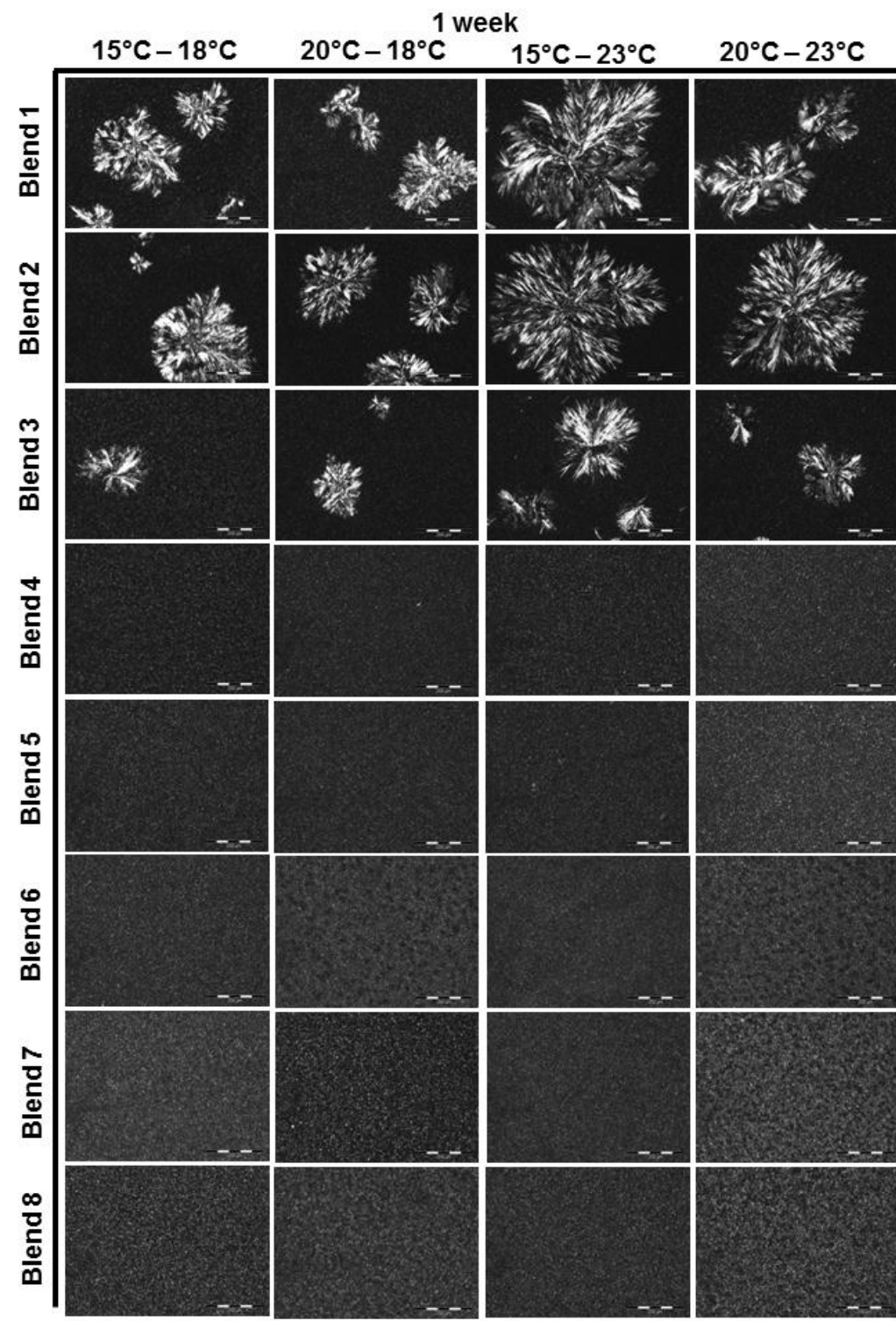


Figure 26 – Microscopic images of all the blends crystallized at 15 and 20°C and stored at 18 and 23°C after a storage period of 1 week.

6.4.2.2. Crystal Growth with time

Figure 27 and 28 demonstrate the pictures taken at different storage times when crystallized and stored at 15°C and 18°C and at 20°C at 18°C, respectively.

Results and Discussion

An important insight from the pictures below is that fat crystals with the spherulitic form are only observed after one week for the blends 1, 2 and 3. Before that period, many small fat crystals with very small gaps between them can be observed.

There are no great changes in the fat networks of the blends with higher SSO content. In general, the networks are composed of many small and densely-packed crystals. A small increase in the size of the crystals can be observed for the blends 6, 7 and 8 that were crystallized at 20°C after 1 week and 1 month of being stored at 18°C.

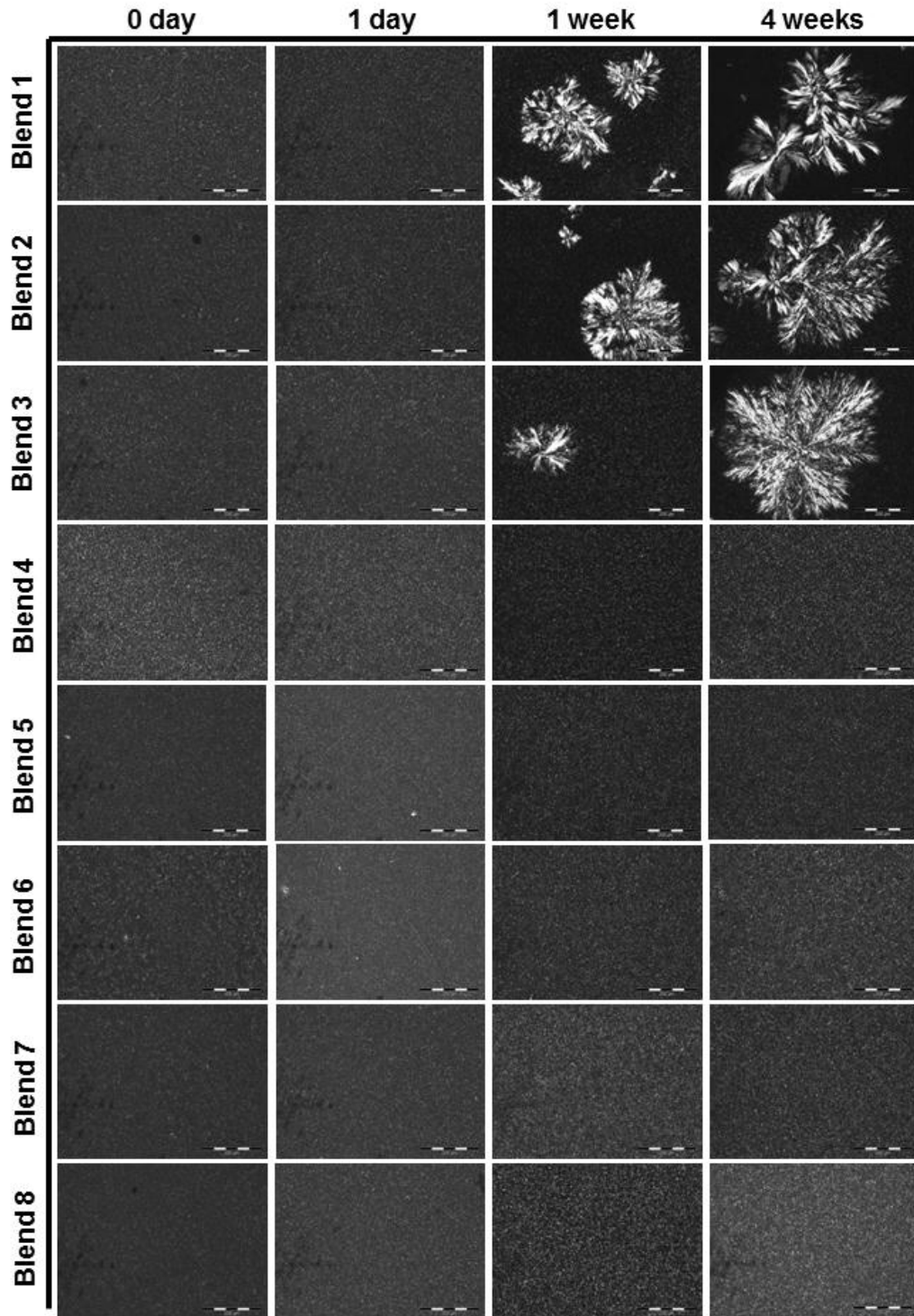


Figure 27 - Microscopic images of all the blends crystallized at 15°C and stored at 18°C.

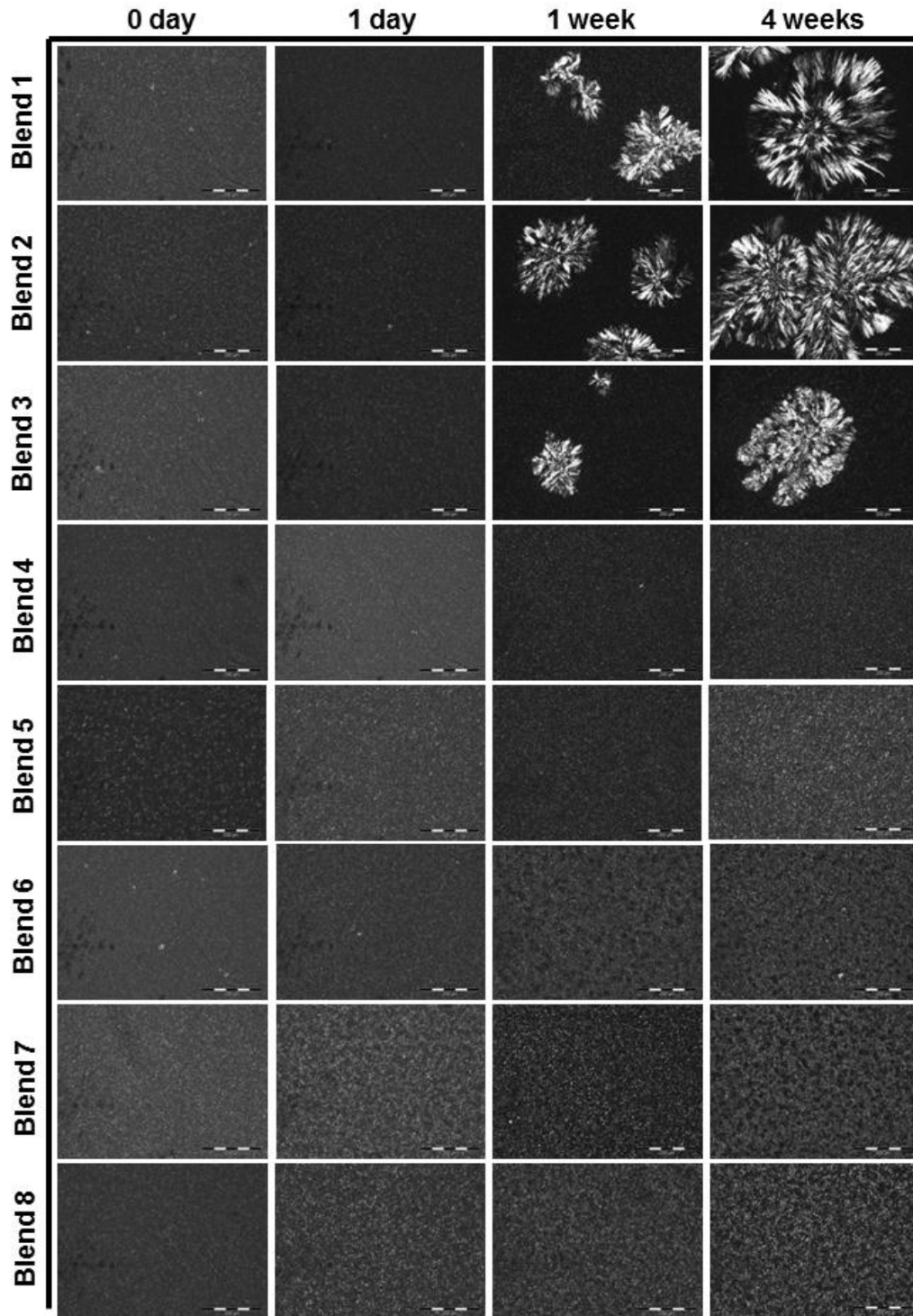


Figure 28 - Microscopic images of all the blends crystallized at 20°C and stored at 18°C.

6.5. Fat migration

One of the main problems with fat-based composite products (e.g. chocolates and pralines) is the oil migration from the filling to the chocolate [REF]. This migration leads to many undesired changes in the texture and organoleptic characteristics of the product [REF]. In this study tempered and untempered samples of the stearic-based blends were placed in contact with hazelnut filling. The samples were stored at 20 and 23°C and the composition of the fat disks was determined after 2, 4, 6, 8, 10 and 16 weeks of storage. The melting profile of the samples was also studied.

6.5.1. Determination of fat migration

In figure 29, an overlay of the TAG profiles with the hazelnut filling and blend 1 at two different periods of the experiment can be observed. In studies of fat migration using hazelnut filling the triacylglycerols LOO, OOO and POO are commonly used to assess the rate and amount of migration that occurs [REF]. Because there are many unsaturated fatty acids in these triacylglycerols, they have a low melting which gives them the ability to migrate from a compound with high concentration of low melting TAG (e.g. the hazelnut filling) to a compound with high melting TAG (e.g. chocolate) [REF]. However, it is important to keep in mind that as the prepared blends already have a considerable amount of OOO (from the addition of high oleic sunflower oil) the migration of this triacylglycerol might be limited.

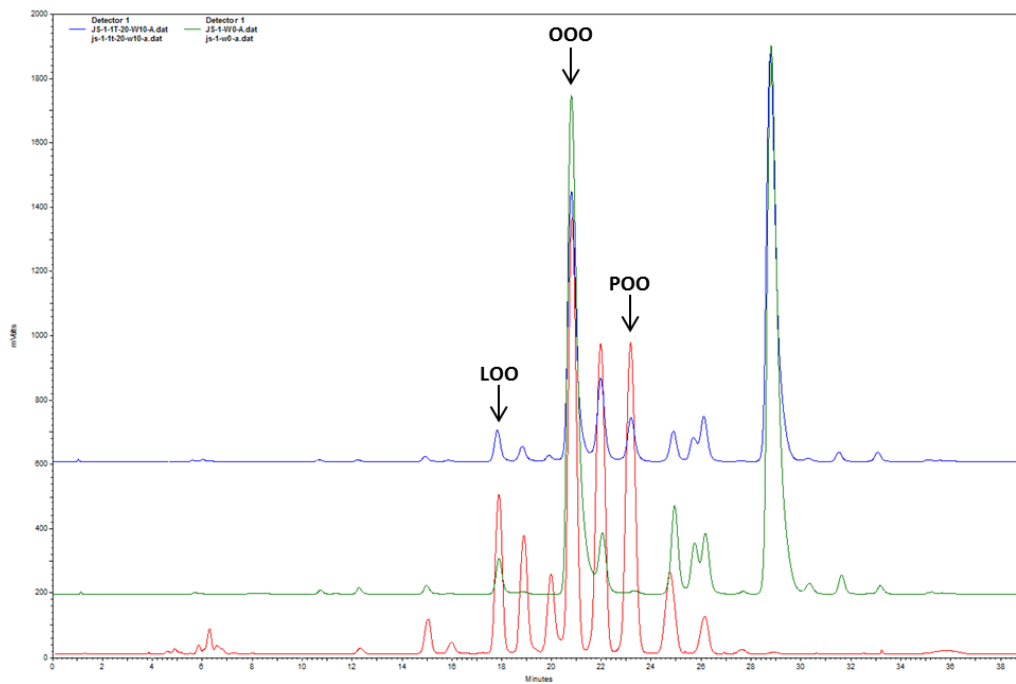


Figure 29 - Overlay of the TAG profile of the hazelnut filling (red), blend 1 (green) and the tempered sample of blend 1 after being stored for 10 weeks at 20°C (blue).

Results and Discussion

By observing figure 30 it is evident that the concentration of all the TAG referenced below increases with time, independently of being tempered or untempered or being stored at 20 or 23°C. However, the values are generally higher for the blends stored at 23°C. This is expected considering that the migrating TAG have low melting points and the higher the storage temperature, the higher will be the capacity of those TAG to migrate.

A curious observation is that, excluding blend 1, the effect of tempering on the prevention of the migration of the TAG after 16 weeks of storage seems to be almost negligible, in some cases the concentration of TAG is even higher in the tempered samples. However, in blend 1 the effect of tempering the blend is much more evident, mainly on the prevention of the migration of POO, LOO, PLO and PLP. There might be many explanations for such occurrences. One of the possible explanations may be related to the polymorphic forms that occur in each of the blends. From the results of XRD it was observed that blend 1 was the only blend where the β polymorph was observed when crystallized at 15°C, at the same temperature the α polymorphic form was present for blend 4 and 6 and α and β' occurred with blend 8. The higher stability of the β polymorph may prevent the migration of low melting triacylglycerols to the stearic-based blend. Another reason may be related to the fact the composition of blend 1 is not as wide as the other three blends, the mixed crystals formed in blend 4, 6 and 8 may have lower stability facilitating the migration of TAG.

Results and Discussion

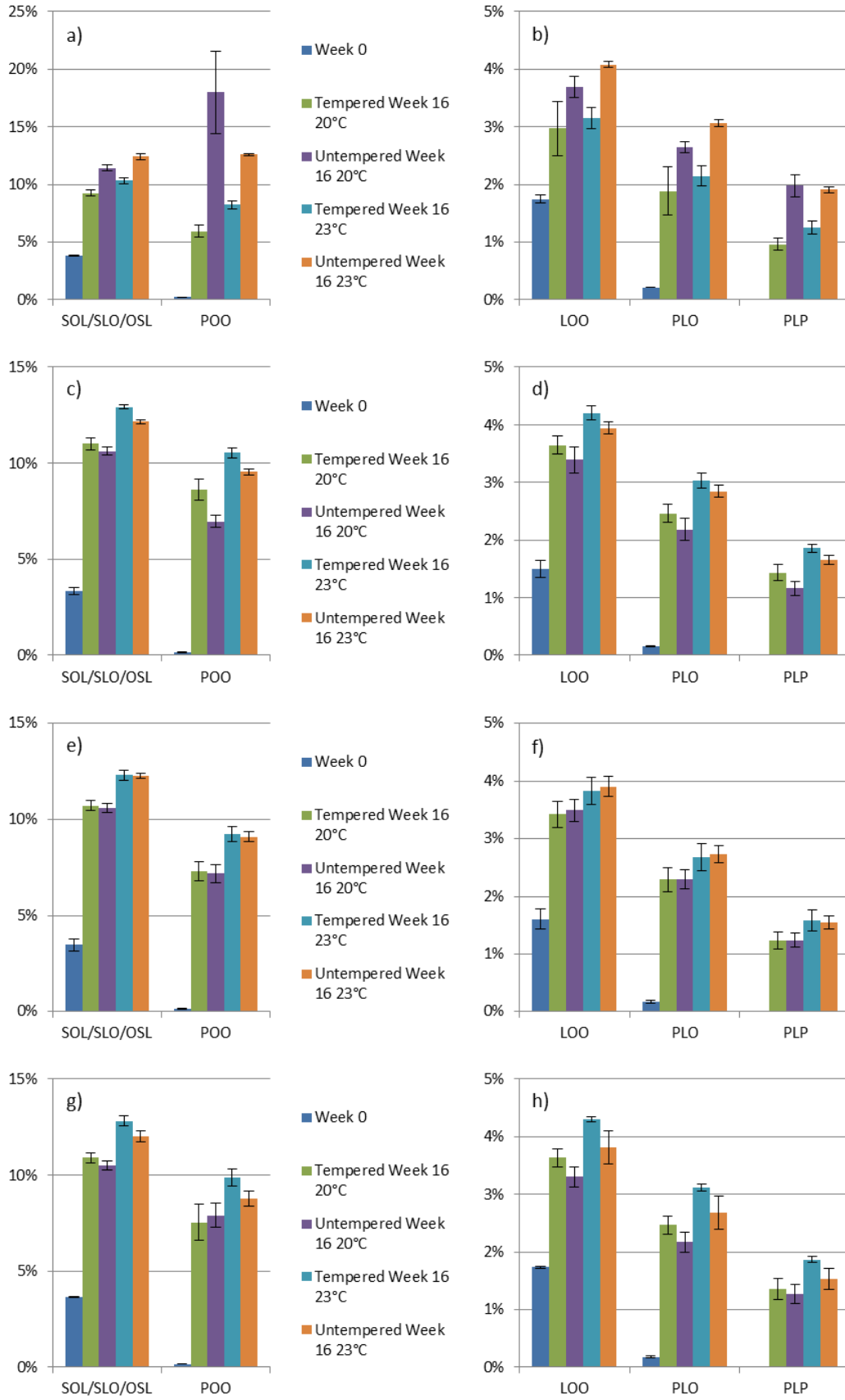


Figure 30 - Comparison of the concentration of various triacylglycerols after 16 weeks of storage for blend 1 (a and b), blend 4 (c and d), blend 6 (e and f) and blend 8 (g and h).

Results and Discussion

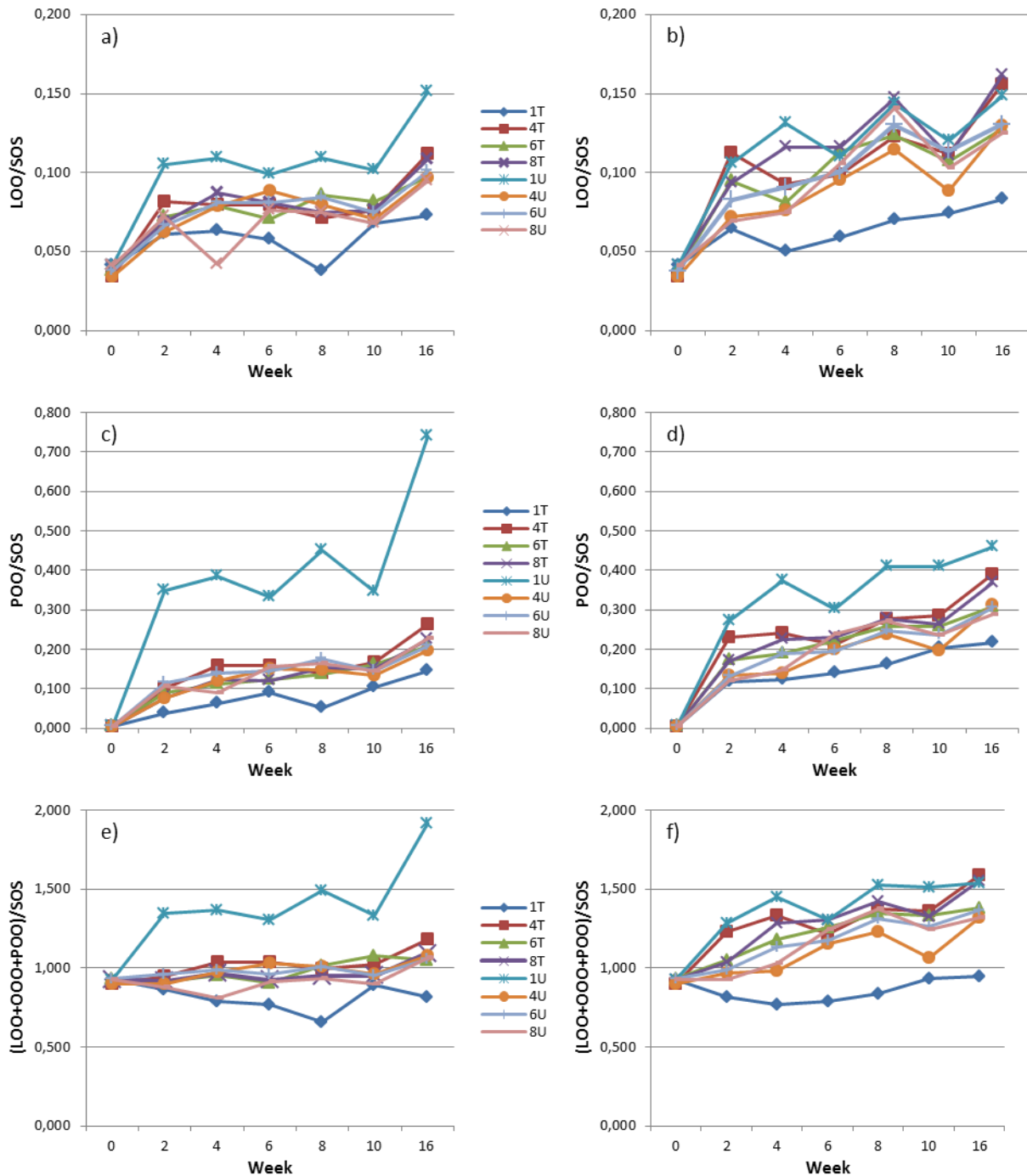


Figure 31 – [LOO/SOS], [POO/SOS] and [(LOO+OOO+POO)/SOS] in layer 2 as function of storage time for blends 1, 4, 6 and 8 both tempered (T) and untempered (U) at storage temperature of 20°C (a, c and e) and 23°C (b, d and f).

The analysis of the various ratios in figure 31 can give further insights about the migration of triacylglycerols during the whole experiment. In general, there is an increase of all of the ratios during all the 16 weeks of the experiment which suggests that there is an overall increase of the migrating TAG over the quantity of SOS present in the blends. This trend occurs for both tempered and untempered samples at any of the storage temperatures.

It is interesting to notice that the ratios of the tempered and untempered samples of blend 1 resulted in the lowest and highest values of all of the gathered values. This means that between

Results and Discussion

all of the blends, the tempered samples of blend 1 were the most effective in preventing the migration of TAG from the hazelnut filling to the stearic-based blend, while the untempered blend 1 was the less effective of them all. The differences in values between the tempered and untempered samples of blend 1 are quite high, but this is not observed for the other blends as the values are quite close to each other. This is strong evidence to support the idea that the composition by itself is enough to prevent the migration of fat. The tempering of the blend may have facilitated the formation of more stable polymorphic forms which had a strong influence on the properties of the fat.

Such effectiveness between the tempered and untempered sample doesn't seem to apply to the other blends. For example, the tempered sample of blend 4 demonstrates higher values than its untempered form. This is more evident when the storage temperature is higher as it can be seen in figure 31b, 31d and 31f. The same results can also be observed for blend 8, which suggests that this is also applicable for blends with high content of SSO.

At the time this document was written no similar studies were done on stearic-based blends which may corroborate these findings. Previous studies on chocolate models reported a positive correlation between the storage temperature and fat migration [27, 48].

The melting profile of the blends was obtained and can be observed in figure 32 and 33. The values of the melting enthalpy can be found in appendix. There was no clear trend that could be observed from the data besides that the values of the melting enthalpy of the tempered samples of blend 1 showed an increasing trend with time, while the untempered sample showed a decreasing trend.

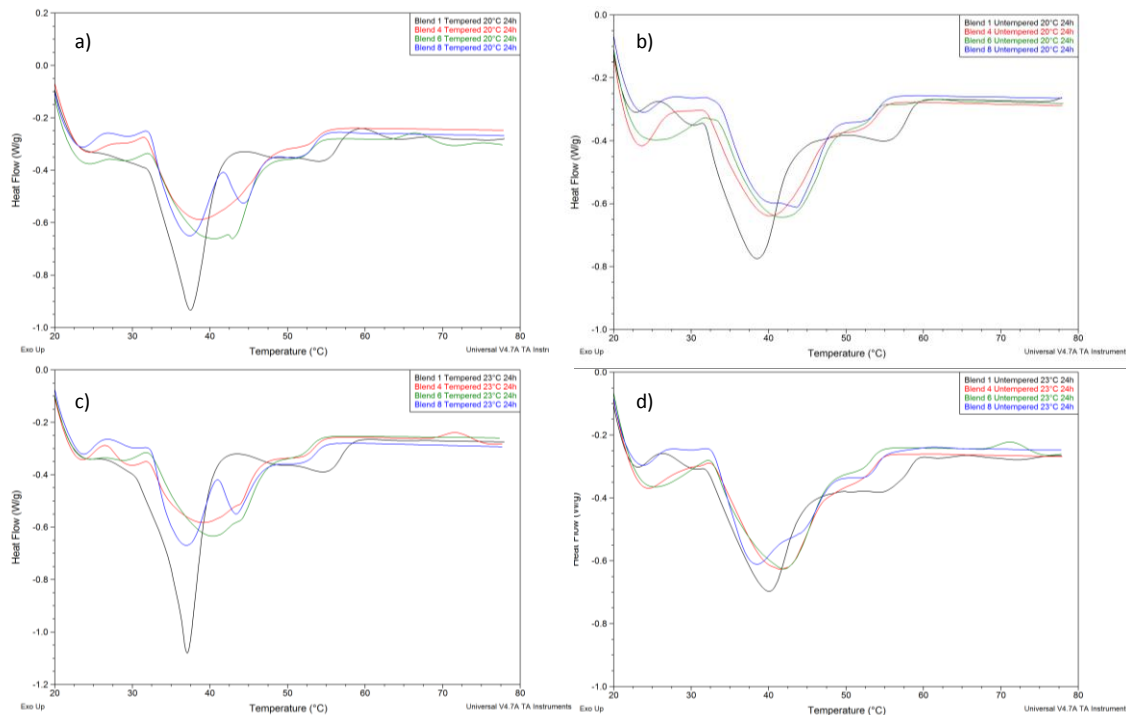


Figure 32 - Melting Profile of the blends 24h after being prepared and stored, a) tempered samples stored at 20°C, b) untempered samples stored at 20°C, c) tempered samples stored at 23°C, d) untempered samples stored at 23°C

Results and Discussion

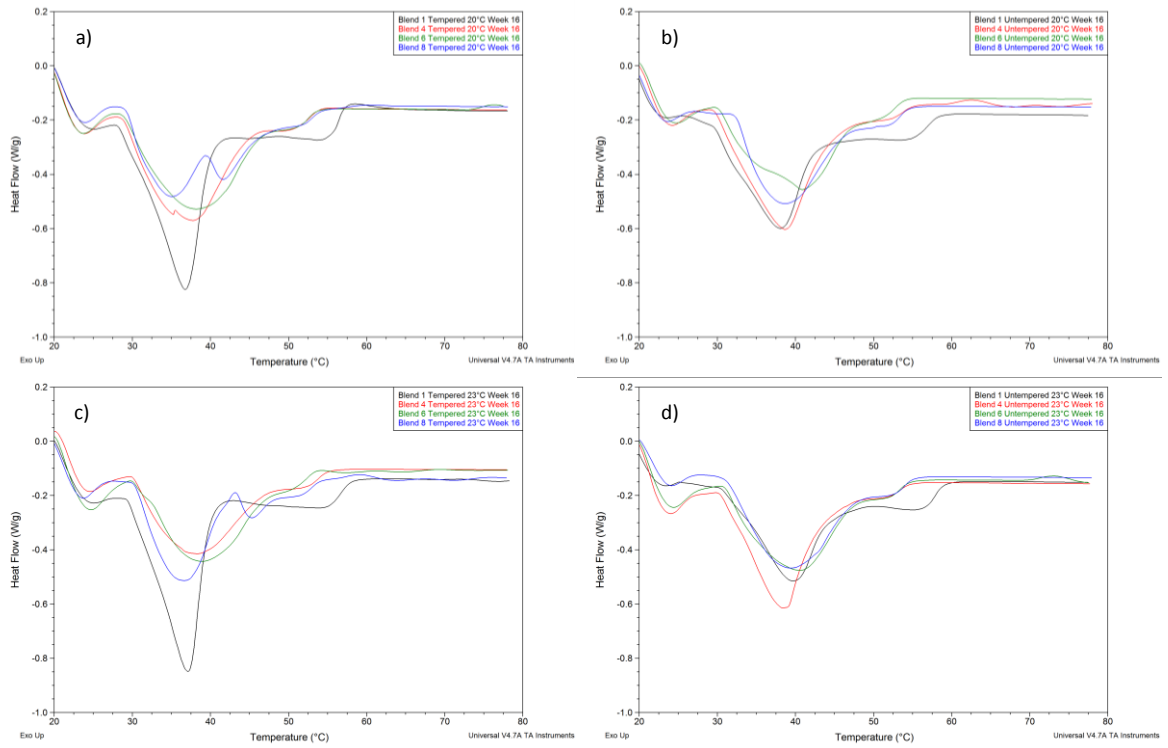


Figure 33 - Melting Profile of the blends after 16 weeks stored, a) tempered samples stored at 20°C, b) untempered samples stored at 20°C, c) tempered samples stored at 23°C, d) untempered samples stored at 23°C

7. Conclusion

The main objective of this thesis was to study the effect of the ratio of symmetric/asymmetric triacylglycerols of stearic-based blends on the crystallization behaviour, the storage stability and the fat migration. In order to do so, eight blends made from different fractions of shea butter and high oleic sunflower oil were prepared with varying ratios of SOS/SSO and equal amount of saturated fatty acids (40%). The ratio of SOS/SSO decreased from blend 1 to blend 8. Samples of the blends were crystallized at 15°C and 20°C and stored at 18°C and 23°C. The research consisted of four parts: the first part studied the composition of the starting materials and blends, the second the crystallization behaviour of the blends, the third the storage stability and the fourth the fat migration of fat from hazelnut filling to tempered and untempered samples of the blends.

In the first part, the HPLC and GC analysis determined the composition of the starting materials and the blends leading to the preparation of the eight blends with decreasing ratio of symmetric/asymmetric TAG and equal amount of saturated fatty acids.

In the second part, the SFC analysis demonstrated that there was no clear trend regarding to the rate of increase of SFC and SFC value with the ratio of symmetric/asymmetric TAG. At all temperatures, a two-step crystallization process could be observed at the various temperatures. In the first step, the SFC increased almost immediately reaching a first plateau. Afterwards, the SFC increased again in a second step and reaches a plateau again where it stabilized until the end of the experiment. At all temperatures blend 1 and 2 crystallized quicker and reached equilibrium before the other blends.

From the DSC data it was shown a shift to higher isothermal times going from blend 1 to 8. The width of the peaks of blend 1 and 2 was lower than the other blends, which may result from the higher amount of symmetric triacylglycerols which due to their higher melting point results in a higher driving force. Independently of the temperature blend 1 crystallized faster than the other blends, demonstrating that symmetric TAG based blends influence positively the rate of crystallization. Interestingly, blend 1 is followed by blend 8. A two-step crystallization process can be observed for all blends.

The XRD data showed a polymorphic transition from α to β and α to β' for blend 1 at 15°C and 20°C, respectively. Regarding to blend 4, only α occurred at 15°C but at 20°C there is a transition from α to β . With blend 6, the α form occurred at 15°C, and at 20°C a transition from α to β is observed, while for blend 8 α to β' transition occurs for both crystallization temperatures.

Conclusion

In the third part, the hardness measurements showed that there was no direct pattern regarding the evolution of the hardness with time and/or ratio of symmetric/asymmetric TAG. It was observed that the two blends with the highest amount of SSO had the highest value of hardness directly after the crystallization at 15°C and the value drops substantially during storage whether it was stored at 18 or 23°C. The obtained values suggest that no post-hardening occurred. The overall effect of the storage temperature on the blends is that there is a decrease in hardness when storing at 23°C when compared to storing at 18°C.

Through polarized light microscopy it was observed that blends 1, 2 and 3 formed big crystals imbedded in a matrix of small crystals, independently of the crystallization and storage temperature. Regarding to the other blends, they presented numerous crystals of very small size and very small gaps between them.

The study of the fat migration was the fourth part of this study and it could be observed that the concentration of POO, LOO, PLO and other TAG increased with time, independently of the samples being tempered or untempered or being stored at 20 or 23°C. However, the values are generally higher for the blends stored at 23°C. Excluding blend 1, the effect of tempering on the prevention of the migration of the TAG after 16 weeks of storage seemed to be almost negligible, in some cases the concentration of TAG was even higher in the tempered samples. Between all of the blends, the tempered samples of blend 1 were the most effective in preventing the migration of TAG from the hazelnut filling to the stearic-based blend, while the untempered blend 1 was the less effective of them all.

8. Further research

The fat migration experiments already gave some insights about the effect of the ratio of symmetric/asymmetric TAG and tempering on the migration of TAG from the hazelnut filling to the fat samples. Further research could be done with the incorporation of part of the stearic based-blends on chocolate models in order to assess the effect these blends on the prevention of fat migration and fat bloom.

It would also be interesting to study the evolution of the fat crystal network, hardness and occurrence of polymorphic forms during migration in order to have more insights on how increasing concentrations of low-melting TAG from hazelnut filling affects those parameters.

Interesting results might also be obtained from the optimization of the tempering process, as it would not only increase the effectiveness of the prevention of fat migration but would also give more insights on the migration process itself.

As there is a growing interest in turning food products healthier, similar research as it was done in this thesis could be done with blends with lower amounts of saturated fatty acids.

Finally, the hardness measurements were unable to detect differences with high accuracy. Although these type of measurement is quite commonly used in the study of fats. The formation of cracks and holes in the samples were observed during the penetration of the probe in the blend which appeared to lead to significant changes in the maximum load profile of the samples and therefore the maximum load value. Therefore the optimization of the process of hardness measurement might be necessary for the study of stearic-based blends.

9. References

1. Hu, F.B., J.E. Manson, and W.C. Willett, *Types of Dietary Fat and Risk of Coronary Heart Disease: A Critical Review*. Journal of the American College of Nutrition, 2001. **20**(1): p. 5-19.
2. Kromhout, D., et al., *Dietary Saturated and transFatty Acids and Cholesterol and 25-Year Mortality from Coronary Heart Disease: The Seven Countries Study*. Preventive Medicine, 1995. **24**(3): p. 308-315.
3. Gunstone, F.D., *The Chemical Nature of Lipids*, in *Oils and Fats in the Food Industry*2008, Wiley-Blackwell. p. 1-10.
4. Scrimgeour, C., *Chemistry of Fatty Acids*, in *Bailey's industrial oil & fats products* F. Shahidi, Editor 2004, Wiley-Interscience.
5. Scrimgeour, C.M., Harwood, J.L. , *Fatty Acid And Lipid Structure*, in *The lipid handbook*, F.D. Gunstone, Harwood, J. L., Dijkstra, A.J., Editor 2007, CRC Press p. 1-36.
6. Scrimgeour, C.M., Harwood, J.L., *Fatty acid and lipid structure*, in *The Lipid Handbook*, F.D. Gunstone, Harwood, J.L., Dijkstra, A.J., Editor 2007, CRC Press. p. 1-16.
7. Foubert, I., Dewettinck, K., Van de Walle, D., Dijkstra, A. J., Quinn P.J., *Physical Properties: Structural and Physical Characteristics*, in *The lipid handbook* F.D. Gunstone, Harwood, J.L., Dijkstra, A.J., Editor 2007, CRC Press. p. 471-495.
8. Metin, S., Hartel, R.W., *Crystallization of Fats and Oils*, in *Bailey's industrial oil & fats products*, F. Shahidi, Editor 2004, Wiley-Interscience.
9. Jones, A.G., *Particulate Crystal Characteristics*, in *Crystallization Process Systems*2002, Butterworth-Heinemann. p. 1-25.
10. Lawler, P.J., Dimick, P.S., *Crystallization and Polymorphism of Fats*, in *Food Lipids: Chemistry, Nutrition, and Biotechnology*, C.C. Akoh, Min, D.B., Editor 2002, Dekker.
11. Jones, A.G., *Crystal formation and breakage*, in *Crystallization Process Systems*2002, Butterworth-Heinemann. p. 123-151.
12. Boistelle, R., *Fundamentals of Nucleation and Crystal Growth*, in *Crystallization and Polymorphism of Fats and Fatty Acids*, N. Garti, Sato, K., Editor 1988, Marcel Dekker: New York. p. 189–226.
13. Garti, N. and K. Satō, *Crystallization processes in fats and lipid systems*2001: Marcel Dekker.
14. Himawan, C., V.M. Starov, and A.G.F. Stapley, *Thermodynamic and kinetic aspects of fat crystallization*. Advances in Colloid and Interface Science, 2006. **122**(1-3): p. 3-33.
15. Modell, M., Reid, R.C. , *Thermodynamics and Its Applications in Chemical Engineering*1974, Englewood Cliffs, NJ: Prentice-Hall.
16. Minato, A., et al., *Synchrotron radiation X-ray diffraction study on phase behavior of PPP-POP binary mixtures*. Journal of the American Oil Chemists' Society, 1996. **73**(11): p. 1567-1572.
17. Himawan, C., V.M. Starov, and A.G.F. Stapley, *Thermodynamic and kinetic aspects of fat crystallization*. Advances in Colloid and Interface Science, 2006. **122**(1–3): p. 3-33.
18. Takeuchi, M., S. Ueno, and K. Sato, *Crystallization kinetics of polymorphic forms of a molecular compound constructed by SOS (1,3-distearoyl-2-oleoyl-sn-glycerol) and SSO (1,2-distearoyl-3-oleoyl-rac-glycerol)*. Food Research International, 2002. **35**(10): p. 919-926.
19. Johansson, D. and B. Bergenståhl, *Sintering of fat crystal networks in oil during post-crystallization processes*. Journal of the American Oil Chemists' Society, 1995. **72**(8): p. 911-920.
20. Johansson, D., *The influence of temperature on interactions and structures in semisolid fats*. Journal of the American Oil Chemists' Society, 1995. **72**(10): p. 1091-1099.

References

21. Laia, O.M., et al., *Physical and textural properties of an experimental table margarine prepared from lipase-catalysed transesterified palm stearin: palm kernel olein mixture during storage*. Food Chemistry, 2000. **71**(2): p. 173-179.
22. Martini, S. and M.L. Herrera, *Physical properties of shortenings with low-trans fatty acids as affected by emulsifiers and storage conditions*. European Journal of Lipid Science and Technology, 2008. **110**(2): p. 172-182.
23. Talbot, G., *Fat migration in biscuits and confectionery systems*. Confectionery Production, 1990. **56**: p. 265-272.
24. Timms, R.E., *Interactions between fats, bloom and rancidity*, in *Confectionery fats handbook. Properties, production and application*, R.E. Timms, Editor 2003, Bridgwater: The Oily Press. p. 255–294.
25. Talbot, G., Smith, K., Zand, T., *Oil Migration: The Basics*, in *Kennedy's Confection* 2006. p. 48-51.
26. Aguilera, J.M., M. Michel, and G. Mayor, *Fat Migration in Chocolate: Diffusion or Capillary Flow in a Particulate Solid?—A Hypothesis Paper*. Journal of Food Science, 2004. **69**(7): p. 167-174.
27. Ali, A., et al., *Effect of storage temperature on texture, polymorphic structure, bloom formation and sensory attributes of filled dark chocolate*. Food Chemistry, 2001. **72**(4): p. 491-497.
28. Depypere, F., et al., *Triacylglycerol migration and bloom in filled chocolates: Effects of low-temperature storage*. European Journal of Lipid Science and Technology, 2009. **111**(3): p. 280-289.
29. Ghosh, V., G.R. Ziegler, and R.C. Anantheswaran, *Fat, Moisture, and Ethanol Migration through Chocolates and Confectionery Coatings*. Critical Reviews in Food Science and Nutrition, 2002. **42**(6): p. 583-626.
30. Dibildox-Alvarado, E., et al., *Effects of Crystalline Microstructure on Oil Migration in a Semisolid Fat Matrix*. Crystal Growth & Design, 2004. **4**(4): p. 731-736.
31. Souleymane, L.C., *The Effect of Symmetric and Asymmetric Triacylglycerol Ratio on the Crystallization Properties and Storage Stability of Model Fat Blends*, in *Food Safety and Food Quality* 2009, Ghent University: Ghent.
32. De Cock, N., *Structure Development in Confectionery Products: Importance of Triacylglycerol Composition in Food Safety and Food Quality* 2011, Ghent University: Ghent.
33. De Cock, N., *Structure development in confectionery products: importance of triacylglycerol composition in Food safety and food quality* 2011, Ghent University.
34. Vereecken, J., et al., *Crystallization of model fat blends containing symmetric and asymmetric monounsaturated triacylglycerols*. European Journal of Lipid Science and Technology, 2010. **112**(2): p. 233-245.
35. Foubert, I., P.A. Vanrolleghem, and K. Dewettinck,, *A differential scanning calorimetry method to determine the isothermal crystallization kinetics of cocoa butter*. Thermochemica Acta, 2003. **400**(1-2): p. 131-142.
36. Foubert, I., et al., *Stop-and-return DSC method to study fat crystallization*. Thermochemica Acta, 2008. **471**(1-2): p. 7-13.
37. Instruments, O. *Solid fat content in edible oils and fats by the direct method (AOCS Cd 16b-93)*. 2009 [cited 2011; Available from: www.oxford-instruments.com].
38. Vereecken, J., *Effect of acylglycerol composition on the microstructural and functional properties of bakery fats and margarines*, in *Food safety and food quality* 2010, Ghent University: Ghent. p. 251.

References

39. Vereecken, J., et al., *Relationship between crystallization behavior, microstructure, and macroscopic properties in trans-containing and trans-free filling fats and fillings*. Journal of Agricultural and Food Chemistry, 2007. **55**(19): p. 7793.
40. Smith, K.W., Cain, F.W., Talbott, G., *Effect of nut oil migration on polymorphic transformation in a model system*. Food Chemistry, 2007. **102**: p. 656-663.
41. Minato, A., et al., , *Thermodynamic and kinetic study on phase behavior of binary mixtures of POP and PPO forming molecular compound systems*. Journal of Physical Chemistry, 1997. **101**(18): p. 3498-3505.
42. Himawan, C., Starov, V.M. , and Stapley, A.G.F.,, *Thermodynamic and kinetic aspects of fat crystallization*. Advances in Colloid and Interface Science, 2006. **122**(1-3): p. 3-33.
43. Vereecken, J., et al., *Effect of SatSatSat and SatOSat on crystallization of model fat blends*. European Journal of Lipid Science and Technology, 2009. **111**(3): p. 243-258.
44. Vereecken, J., et al., *Effect of TAG composition on the crystallization behaviour of model fat blends with the same saturated fat content*. Food Research International, 2010. **43**(8): p. 2057-2067.
45. Jacobsberg, B. and O.C.H. Oh Chuan Ho, *Studies in palm oil crystallization*. Journal of the American Oil Chemists' Society, 1976. **53**(10): p. 609-617.
46. Engstrom, L., *Triglyceride systems forming molecular compounds*. J. Fat Sci. Technol., 1992. **94**: p. 173-181.
47. Hagemann, J.W., in *Crystallization and Polymorphism of Fats and Fatty Acids*, N. Garti, Sato, K. , Editor 1988, Marcel Dekker Inc. p. 9-95.
48. Miquel, M.E., Carli, S., Couzens, P.J., Wille, H., Hall, L.D. , *Kinetics of the migration of lipids in composite chocolate measured by magnetic resonance imaging*. Food Research International, 2001. **34**: p. 773-781.

10. Appendices

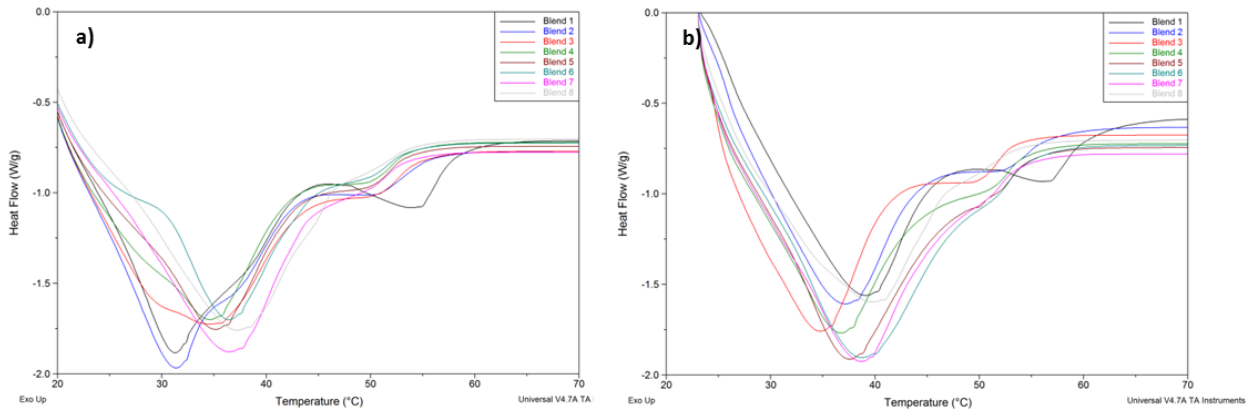


Figure 34 - Melting profiles at a) 18°C and at b) 23°C.

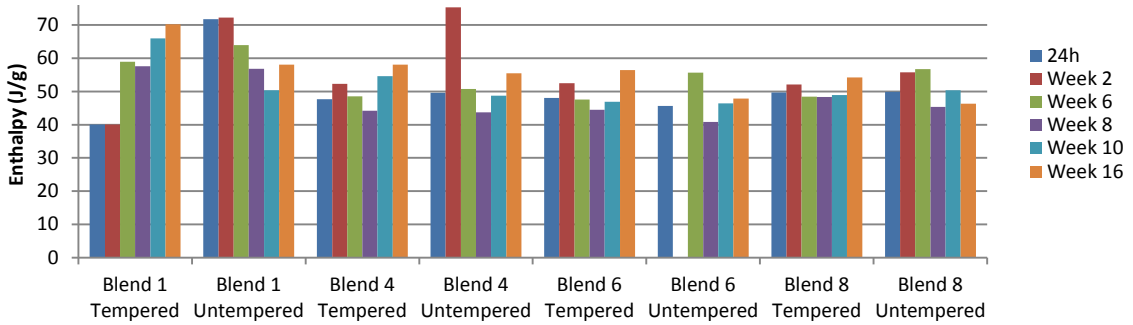


Figure 36 - Melting enthalpy of the blends stored at 20°C.

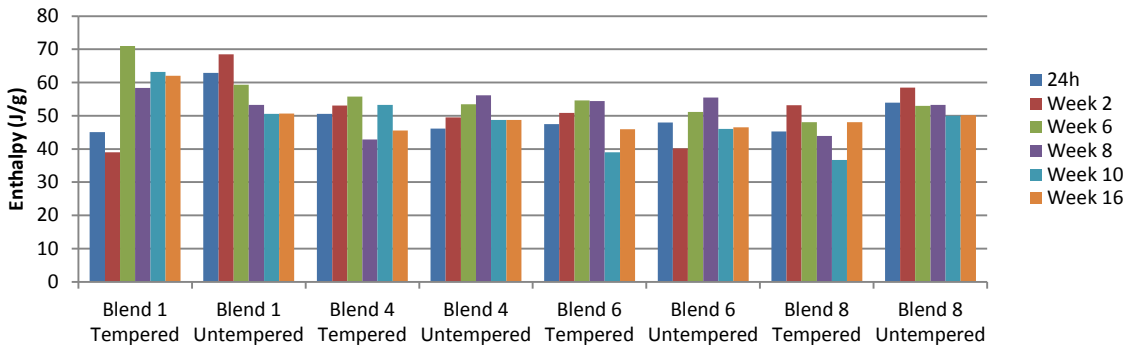


Figure 35 - Melting enthalpy of the blends stored at 23°C.